Molecular Biology of the Cell
Vol. 15, 371–383, January 2004

# The Calcium Binding Loops of the Cytosolic Phospholipase $A_2$ C2 Domain Specify Targeting to Golgi and ER in Live Cells[V]

**John H. Evans,* Stefan H. Gerber,† Diana Murray,‡ and Christina C. Leslie*§**

*Program in Cell Biology, Department of Pediatrics, National Jewish Medical and Research Center, Denver, Colorado 80206, and Departments of Pathology and Pharmacology, University of Colorado School of Medicine, Denver, Colorado 80262; †Department of Cardiology, University of Heidelberg, 69115 Heidelberg, Germany; and ‡Department of Microbiology and Immunology, Weill Medical College of Cornell University, New York, New York 10021

Submitted May 28, 2003; Revised August 6, 2003; Accepted August 26, 2003
Monitoring Editor: Vivek Malhotra

**Translocation of cytosolic phospholipase $A_2$ ($cPLA_2$) to Golgi and ER in response to intracellular calcium mobilization is regulated by its calcium-dependent lipid-binding, or C2, domain. Although well studied in vitro, the biochemical characteristics of the $cPLA_2$C2 domain offer no predictive value in determining its intracellular targeting. To understand the molecular basis for $cPLA_2$C2 targeting in vivo, the intracellular targets of the synaptotagmin 1 C2A (Syt1C2A) and protein kinase C$\alpha$ C2 (PKC$\alpha$C2) domains were identified in Madin-Darby canine kidney cells and compared with that of hybrid C2 domains containing the calcium binding loops from $cPLA_2$C2 on Syt1C2A and PKC$\alpha$C2 domain backbones. In response to an intracellular calcium increase, PKC$\alpha$C2 targeted plasma membrane regions rich in phosphatidylinositol-4,5-bisphosphate, and Syt1C2A displayed a biphasic targeting pattern, first targeting phosphatidylinositol-4,5-bisphosphate-rich regions in the plasma membrane and then the *trans*-Golgi network. In contrast, the Syt1C2A/$cPLA_2$C2 and PKC$\alpha$C2/$cPLA_2$C2 hybrids targeted Golgi/ER and colocalized with $cPLA_2$C2. The electrostatic properties of these hybrids suggested that the membrane binding mechanism was similar to $cPLA_2$C2, but not PKC$\alpha$C2 or Syt1C2A. These results suggest that primarily calcium binding loops 1 and 3 encode structural information specifying Golgi/ER targeting of $cPLA_2$C2 and the hybrid domains.**

## INTRODUCTION

Correct spatiotemporal targeting of proteins to specific cellular sites is critical in the regulation of cell signaling (Teruel and Meyer, 2000), and many cytoplasmic signaling proteins that function at membrane surfaces rely on modular domains, such as C2, pleckstrin homology (PH), Phox, FYVE, and ENTH domains (Rizo and Sudhof, 1998; Itoh and Takenawa, 2002) for their targeting. Of these, C2 domains differ by responding to intracellular $Ca^{2+}$ signals, thus providing a link between receptor-mediated $Ca^{2+}$ signals and interaction of host proteins with membrane (Oancea and Meyer, 1998; Teruel and Meyer, 2002).

In response to intracellular $Ca^{2+}$ signals, $cPLA_2$ translocates to Golgi and ER where it catalyzes the release of arachidonic acid (AA) from phospholipids (Glover *et al*., 1995; Schievella *et al*., 1995; Hirabayashi *et al*., 1999; Perisic *et al*., 1999; Choukroun *et al*., 2000; Evans *et al*., 2001). Targeting specificity and sensitivity to $Ca^{2+}$ is provided to the intact enzyme by its N-terminal C2 domain (Nalefski *et al*., 1994; Perisic *et al*., 1998; Dessen *et al*., 1999; Gijón *et al*., 1999; Hirabayashi *et al*., 1999; Perisic *et al*., 1999; Evans *et al*., 2001), which is similar to C2 domains from other signaling proteins, such as PKC$\alpha$ and Syt1 (Sutton *et al*., 1995; Nalefski and Falke, 1996; Shao *et al*., 1998; Verdaguer *et al*., 1999) (Figure 1, A and B). C2 domains are composed of ~130 amino acids that fold into a $\beta$ sandwich structure and are found in two topologies (types I and II) due to a circular permutation in the amino acid sequence (Nalefski and Falke, 1996). Most of the homology among C2 domains is found in the conserved core region that supports the surface-exposed calcium binding loops (CBLs) (Sutton *et al*., 1995). Less homology is found among the CBLs themselves, with $cPLA_2$C2 having a unique $\alpha$-helical region in the first CBL.

For many C2 domains, including PKC$\alpha$C2 and synaptotagmin 1 C2A (Syt1C2A), $Ca^{2+}$ binding results in the negative electrostatic potential in the area of the CBLs becoming positive, thereby promoting electrostatic interactions with negatively charged membranes (Shao *et al*., 1997; Rizo and Sudhof, 1998; Murray and Honig, 2002). As a result, Syt1C2A and PKC$\alpha$C2 preferentially bind to anionic phospholipids, such as phosphatidylserine (PS) and phosphatidylinositolpolyphosphates, but not to phospholipids with neutral headgroups, such as phosphatidylcholine (PC)

Article published online ahead of print. Mol. Biol. Cell 10.1091/mbc.E03–05–0338. Article and publication date are available at www.molbiolcell.org/cgi/doi/10.1091/mbc.E03–05–0338.

[V] Online version of this article contains videos for some figures. Online version is available at www.molbiolcell.org.

§ Corresponding author. E-mail address: lesliec@njc.org.

Abbreviations used: BFA, brefeldin A; $cPLA_2$, cytosolic phospholipase $A_2$; FP, fluorescent protein; GT, $\beta$1,4 galactosyltransferase; IONO, ionomycin; PC, phosphatidylcholine; PH, pleckstrin homology; $PIP_2$, phosphatidylinositol-4,5-bisphosphate; PS, phosphatidylserine; Syt1C2A, synaptotagmin I C2A.

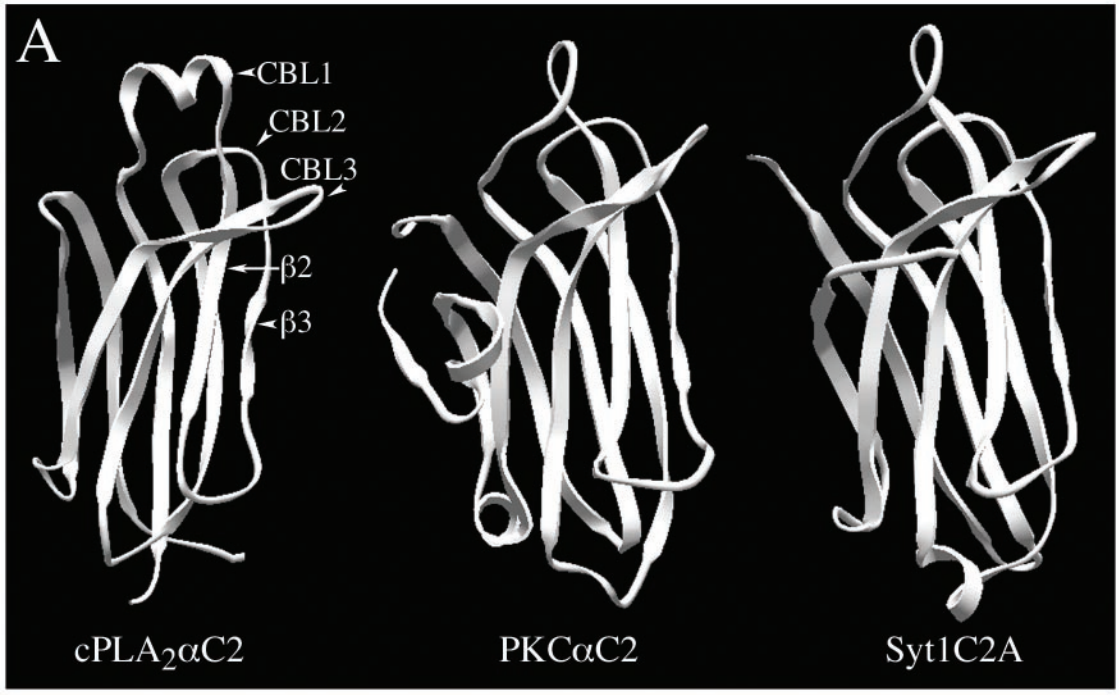


B

```
hcPLA2αC2                SHKFTVVVLRATKVTKGAFG-DMLDTPDPYVELFISTTP--DSRKRTRHFNNDIN
                                   V +R  K        D     DPYV+L +   P  +S+++T+   + +N
hPKCαC2     KRGRIY--LKAEVADEKLHVTVRDAKNLI--PM-DPNGLSDPYVKLKLIPDPKNESKQKTKTIRSTLN
            K G++   L +   + +L V +  A  L   P+ D  G SDPYVK+ L+P+ K   K +TK  R TLN
rSyt1C2A   EKLGKLQYSLDYDFQNNQLLVGIIQAAEL---PALDMGGTSDPYVKVFLLPEKKK--KFETKVHRKTLN

hcPLA2αC2   PVWNETFEFILDP--NQENV-LEITLMDAN-YVM-DETLGTATFTVSS-MKVGEKKEVPFIFNQVTEMVLEMSLEV
            P WNE+F F L P  +++   L + + D +     D  +G+ +F VS  MK+         +
hPKCαC2     PQWNESFTFKLKP-SDKDRR-LSVEIWDWDRTTRND-FMGSLSFGVSELMKMPASG-WYKL
            P +NE FTFK+ P S+   + L + ++D+DR +++D  +G     + +          W  L
rSyt1C2A    PVFNEQFTFKV-PYSELGGKTLVMAVYDFDRFSKHD-IIGEFKVPMNTVDFGHVTEEWRDL
```

**Figure 1.** Structural and sequence comparisons of cPLA$_2$C2, PKC$\alpha$C2, and Syt1C2A domains. (A) Ribbon diagrams of cPLA$_2$C2, PKC$\alpha$C2, and Syt1C2A (Protein Data Bank entries 1RLW, 1DSY, and 1BYN, respectively) show CBLs 1–3 and $\beta$ strands 2 and 3 of cPLA$_2$C2 (homologous to $\beta$ strands 3 and 4 of PKC$\alpha$C2 and Syt1C2A). (B) Amino acid sequence alignment of cPLA$_2$C2 (residues 17–138, AAB00789), PKC$\alpha$C2 (residues 158–277, P17252), and Syt1C2A domains (residues 140–262, P21707). The residues included in the CBLs are shaded in gray and the residues in the conserved core are under the black line.

(Schiavo *et al.*, 1996; Arcaro *et al.*, 1998; Davletov *et al.*, 1998; Zhang *et al.*, 1998; Corbalán-García *et al.*, 1999; Verdaguer *et al.*, 1999; Gerber *et al.*, 2001; Nalefski *et al.*, 2001; Kohout *et al.*, 2002; Ochoa *et al.*, 2002). In contrast to the Syt1C2A and PKC$\alpha$ C2 domains, hydrophobic interactions predominate in the interaction of the cPLA$_2$C2 domain with membranes, and $Ca^{2+}$ binding neutralizes the negative electrostatic potential surrounding hydrophobic residues located at the tips of the cPLA$_2$C2 CBLs 1 and 3, facilitating their penetration into the membrane surface (Davletov *et al.*, 1998; Perisic *et al.*, 1998; Xu *et al.*, 1998; Bittova *et al.*, 1999; Perisic *et al.*, 1999; Gerber *et al.*, 2001; Nalefski *et al.*, 2001). Also, unlike Syt1C2A and PKC$\alpha$C2, cPLA$_2$C2 preferentially binds to lipid vesicles composed entirely of PC (Nalefski *et al.*, 1997; Davletov *et al.*, 1998; Hixon *et al.*, 1998; Nalefski and Falke, 1998; Perisic *et al.*, 1999; Gerber *et al.*, 2001) but can also bind to membranes composed partially, but not entirely, of anionic phospholipids (Davletov *et al.*, 1998; Gerber *et al.*, 2001; Nalefski *et al.*, 2001; Stahelin *et al.*, 2003). The importance of the CBLs in determining membrane-binding properties is exemplified in experiments where the phospholipid preference of Syt1C2A was switched to that of cPLA$_2$C2 by grafting the CBLs of cPLA$_2$C2 onto Syt1C2A (Gerber *et al.*, 2001).

Although much has been learned about the structural characteristics, electrostatic properties, and lipid preferences of C2 domains, the mechanisms by which they target specific membranes in living cells remains unclear. Here, we use an imaging approach to correlate structural features of the cPLA$_2$C2 domain with targeting to Golgi and ER in response to $Ca^{2+}$ mobilization. Using fluorescent protein (FP)-labeled C2 domains having diverse biochemical properties and FP-labeled lipid-specific and organelle-specific probes, we first characterized the spatiotemporal characteristics of cPLA$_2$C2, Syt1C2A, and PKC$\alpha$C2 domain translocation in response to intracellular calcium ($[Ca^{2+}]_i$) increase. We then directly compared targeting between these wild-type C2 domains

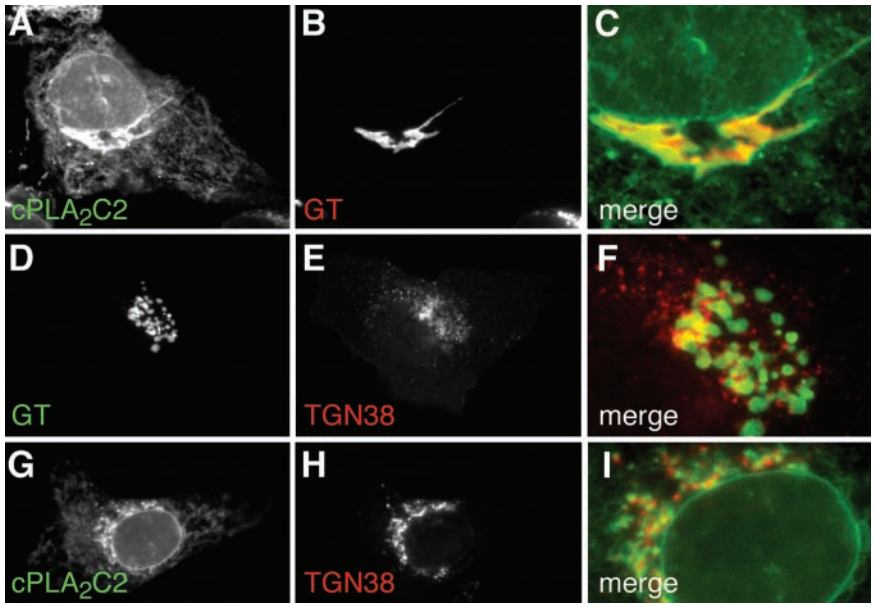


**Figure 2.** The cPLA$_2$ C2 domain targets Golgi and ER. Images of a cell coexpressing (A) EYFP-cPLA$_2$C2 and (B) ECFP-GT at 27 s after treatment with 10 $\mu$M IONO are shown. A merged image (C) shows the region of the Golgi from A and B. Images of a cell coexpressing (D) ECFP-GT and (E) TGN38-EYFP, and (F) a merged image of D and E in the region of TGN and Golgi are shown. Images of cells coexpressing (G) ECFP-cPLA$_2$C2 and (H) TGN38-EYFP at 30 s after treatment with 10 $\mu$M IONO are shown. A merged image (I) shows the region of the TGN. Images are representative of a minimum of five experiments.

and hybrid Syt1C2A/cPLA$_2$C2 and PKC$\alpha$C2/cPLA$_2$C2 domains containing cPLA$_2$C2 CBLs.

## MATERIALS AND METHODS

### *Fluorescent Protein Constructs*

pEGFP-cPLA$_2$C2 encoding the human cPLA$_2$ C2 domain (residues 17–148, accession M72393) fused to enhanced green fluorescent protein (EGFP) was cloned as described previously (Evans *et al.*, 2001). Rat Syt1C2A fused to enhanced yellow fluorescent protein (EYFP) (residues 140–267, pEYFP-Syt1C2A) was constructed by polymerase chain reaction (PCR) amplification of the C2 domain from pGEX65-4 (Nishiki *et al.*, 1994) by using primers Syt1C2Afwd (CGCGGATCCGAAAACTGGGAAAGCTCCAATATTCACTG) and Syt1C2Arev (CCCAAGCTTTTTCTCAGCGCTCTGGAGATCGCGCCACTC), and subcloning the PCR product into the *Bgl*II/*Hind*III site of EYFP(C1). A construct encoding rat Syt1C2A and the three calcium binding loops from rat cPLA$_2$C2 fused to EYFP (pEYFP-Syt1C2A_cPLA$_2$C2_L1.2.3) was constructed by ligating the *Bam*HI/*Hind*III fragment from pGEXSyt1C2A_cPLA$_2\alpha$C2_L1.2.3 (Gerber *et al.*, 2001) into the *Bgl*II/*Hind*III site of EYFP(C1). Human PKC$\alpha$ (accession X52479) fused to EGFP (pEGFP-PKC$\alpha$) was constructed by inserting the EcoR1 fragment from pHACE-PKC$\alpha$, a gift from I. Weinstein (Columbia University, New York, NY), into the EcoR1 site of pEGFP(C2). A construct encoding human PKC$\alpha$ C2 domain (residues 158–286) fused to ECFP (pECFP-PKC$\alpha$C2) was constructed by PCR amplification of pEGFP-PKC$\alpha$ by using primers PKC$\alpha$C2fwd (GTCAAGCTTAAGAGGGGGCGGATTTACCTA) and PKC$\alpha$C2rev (CGTCGACTGGTAGTACTCACCTTCTTCTTG), and cloning the PCR product into the *Hind*III/*Sal*I site of ECFP(C3). pECFP-PKC$\alpha$C2/N189F and pECFP-PKC$\alpha$C2/N189F/T250Y were produced by site-directed mutagenesis (Stratagene, La Jolla, CA). Constructs encoding the human PKC$\alpha$ C2 domain with human cPLA$_2$C2 calcium binding loops 1 and 3 or 1, 2, and 3 (pECFP-PKC$\alpha$C2_cPLA$_2$C2_L1.3 and pECFP-PKC$\alpha$C2_cPLA$_2$C2_L1.2.3, respectively) were assembled from overlapping PCR fragments obtained by amplification of pECFP-PKC$\alpha$C2 with PKC$\alpha$C2fwd, PKC$\alpha$C2rev primers and primers containing the cPLA$_2$C2 loop sequences (PKC$\alpha$C2_cPLA$_2$C2_loop1rev = TGGAGTATCAAGCATGTCACCAAAGGCCCCCTTTGTTAGATTTTTTGCATCTCGTACTGTGACATGGAGC; PKC$\alpha$C2_cPLA$_2$C2_loop1fwd = ACAAAGGGGGCCTTTGGTG-ACATGCTTGATACTCCAGATCCTTATGTGAAGCTGAAACTTATTCCTGATCCC; PKC$\alpha$C2_cPLA$_2$C2_loop2rev = GTTTATGTCATTATTGAAGGTT-TTGGTTTTTTGCTTGC; PKC$\alpha$C2_cPLA$_2$C2_loop2fwd = TTCAATAATGA-CATAAACCCGCAGTGGAATGAGTCC; PKC$\alpha$C2_cPLA$_2$C2_loop3rev = TTCATCCATGACATAATTGGCGTCCCAGATTTCTACAGACAGTCG; PKC$\alpha$C2_cPLA$_2$C2_loop3fwd = GCCAATTATGTCATGGATGAATTCATGGGATCCCTTTCCTTTGG). The fragments were assembled by PCR and cloned into the *Hind*III/*Sma*I site of ECFP(C3). pECFP-GT, which contains the N terminal 82 amino acids of $\beta$-1,4-galactosyltransferase fused to enhanced cyan fluorescent protein (ECFP), was purchased from BD Biosciences Clontech (Palo Alto, CA). TGN38-ECFP and TGN38-EYFP were gifts from K. Simons (Max Planck Institute, Dresden, Germany). EGFP-PLC$\delta_1$PH domain was a gift from M. Lemmon (University of Pennsylvania School of Medicine, Philadelphia, PA). ECFP-Rab5 was a gift from A. Sorkin (University of Colorado Health Sciences Center, Denver, CO). The pEYFP plasmid used in this study was constructed from pEYFP purchased from BD Biosciences Clontech by introducing a Q70M mutation by site-directed mutagenesis (Stratagene) to improve its qualities (Griesbeck *et al.*, 2001). Different fluorescent protein constructs were produced by substituting *Nhe*I/BsrGI fragments encoding the fluorescent protein-encoding region from pECFP and pEYFP. All constructs were confirmed by sequencing.

### *Cell Culture*

MDCK cells obtained from American Type Culture Collection (Manassas, VA) were cultured in DMEM containing 10% fetal bovine serum, 100 U/ml penicillin, 100 $\mu$g/ml streptomycin, 0.292 mg/ml glutamine in 5% $CO_2$ at 37°C. Subconfluent cells ($1 \times 10^4$ cells/cm$^2$) were transfected with the relevant plasmid(s) by using FuGENE-6 (Roche Diagnostics, Indianapolis, IN) in DMEM containing 0.2% bovine serum albumin, 100 U/ml penicillin, 100 $\mu$g/ml streptomycin, 0.292 mg/ml glutamine following the manufacturer's protocol.

### *Microscopy of Fluorescent Proteins*

Transfected Madin-Darby canine kidney (MDCK) cells grown on MatTek plates were washed with and incubated in Hanks' balanced salt solution additionally buffered with 25 mM HEPES, pH 7.4 (HEPES-Hanks' balanced salt solution). Cells were imaged using an Olympus inverted microscope equipped with a 60×, 1.25 numerical aperture oil immersion objective, cyan fluorescent protein (CFP) and yellow fluorescent protein (YFP) emission filters (Chroma Technology, Brattleboro, VT) in a Sutter filter wheel, a CFP/YFP dichroic mirror, and a TILL Imago charge-coupled device camera (TILL Photonics, Gräfelfing, Germany). Excitation light of 430 and 510 nm for CFP and YFP, respectively, was provided using a Polychrome IV monochromator (TILL Photonics). TILLvisION software was used for acquisition and analysis. Final images were produced using Adobe Photoshop.

FP fluorescence with respect to time was determined for regions of interest (ROI) corresponding to the plasma membrane or to *trans*-Golgi network (TGN) by the following method. Background-corrected average pixel values were determined for $ROI_{TGN}$ at each time point. Due to photobleaching during the course of the experiments, bleach correction factors were calculated for each time point by first determining the background-corrected average pixel values for an ROI corresponding to the entire cell ($ROI_{cell}$) and then normalizing those values to the initial value at t = 0. The background- and bleach-corrected fluorescence value, $F_t$, was calculated by dividing the background-corrected average pixel value for each ROI at each time point by the bleach correction factor at the corresponding time point. The normalized fluorescence at the plasma membrane or TGN was calculated by dividing $F_t$ by the t = 0 fluorescence value, $F_0$, to yield $F_t/F_0$.

### *Structural Models*

The Protein Data Bank (Berman *et al.*, 2000) identifiers for the experimentally determined C2 domain structures used in the calculations are as follows: cPLA$_2$C2 (1RLW; Perisic *et al.*, 1998), Syt1C2A (1BYN; Shao *et al.*, 1998), and PKC$\alpha$C2 (1DSY; Verdaguer *et al.*, 1999). It was assumed that the C2 domains

bound the number of calcium ions specified by the structural studies. Specifically, the calcium-bound forms of $cPLA_2C2$, Syt1C2A, and PKCαC2 used in the electrostatic calculations contained two, three, and two calcium ions, respectively. The hybrid C2 domain models illustrated in Figures 4, 9, and 10 were constructed by placing the respective loop regions from $cPLA_2C2$ onto the structural cores of Syt1C2A and PKCαC2. The structures of both Syt1C2A and PKCαC2 were superimposed onto the $cPLA_2C2$ structure by using the program Combinatorial Extension (Shindyalov and Bourne, 1998). Once structurally aligned, the appropriate portions of the $cPLA_2C2$ Protein Data Bank file replaced regions of the Syt1C2A and PKCαC2 Protein Data Bank files as dictated by the sequence alignments depicted in Figures 1, 4, and 9. The hybrid C2 domain models were energy minimized in the program Modeler (Sali and Blundell, 1993) to fix any mismatches between the various structural segments. Because the calcium coordination schemes of the hybrid C2 models are closest to that of $cPLA_2C2$, it was assumed that the hybrid C2 models bind two calcium ions in the same manner as $cPLA_2C2$. The calcium ions were docked onto the hybrid models by structurally superimposing the models onto the experimentally determined structure of $cPLA_2C2$ (1RLW) and transferring the coordinates of the calcium ions from the $cPLA_2C2$ coordinate file to the coordinate files for the models. A model for the N189F/T250Y mutant of PKCαC2 was obtained from the original Protein Data Bank coordinates for PKCαC2 by building in the appropriate side chains at positions 189 and 250 by using the program CHARMM (Brooks *et al.*, 1983). Hydrogen atoms were added to the heavy atoms in the structures and models with CHARMM. The structures with hydrogens were subjected to conjugate gradient minimization with a harmonic restraint force of 50 kcal/mol/Å$^2$ applied to the heavy atoms located at the original crystallographic coordinates.

### *Membrane Models*

A structural model for the 2:1 PC/PS bilayer was built as described previously (Ben-Tal *et al.*, 1996). Because the purpose of the calculations in Table 1 is to quantify the change in the electrostatic free energy of interaction of the C2 domains with charged membrane surfaces, it is assumed that the lipids change neither structure nor position upon interaction with the protein. These approximations are reasonable for the C2 domains from Syt1 and PKCα because both are highly charged and do not penetrate the membrane interface to a large degree. A similar treatment of C2 domains was applied in previous computational work (Murray and Honig, 2002).

### *Electrostatic Calculations*

In Figure 10, the electrostatic properties of the C2 domains of known structure, the PKCaC2/N189F/T250Y mutant, and Syt1C2A/$cPLA_2C2$ and PKCαC2/$cPLA_2C2$ hybrids were calculated for 0.1 M KCl, and visualized in GRASP (Nicholls *et al.*, 1991).

For the calculations depicted in Table 1, the electrostatic potentials and free energies were obtained as described previously (Murray and Honig, 2002). The finite difference Poisson-Boltzmann (FDPB) method has previously been shown to yield excellent agreement with experimental measurements of the binding of peptides and proteins to charged membranes (Ben-Tal *et al.*, 1996, 1997; Murray *et al.*, 1998; Murray and Honig, 2002). Electrostatic free energies are obtained from the calculated potentials (Sharp and Honig, 1990), and the electrostatic free energies of interaction are determined as the difference between the electrostatic free energy of a C2 domain in a specific orientation with respect to the membrane surface, $G_{el}(P{\cdot}M)$, and the electrostatic free energies of the C2 domain, $G_{el}(P)$, and membrane, $G_{el}(M)$, infinitely far apart, i.e., taken separately:

$$\Delta G_{el} = G_{el}(P{\cdot}M) - [G_{el}(P) + G_{el}(M)]$$

The membrane-associated orientations of the calcium-bound Syt1C2A and PKCαC2 domains are the orientations of minimum electrostatic free energy. These were determined by comparing the electrostatic free energies of interaction of different orientations sampled about an orientation obtained by visual inspection of the electrostatic potential profiles in GRASP. Previous work has established that, for peripheral association, both the relative binding free energies and the electrostatic contribution to the absolute binding free energies are well described by consideration of minimum free energy orientation alone (Ben-Tal *et al.*, 1996, 1997; Murray *et al.*, 1998). The membrane-associated orientations of $cPLA_2C2$ and the hybrid models are similar to those of the Syt1C2A and PKCαC2 domains for comparison purposes.

## RESULTS

We first performed experiments to establish the spatiotemporal targeting patterns of three, biochemically diverse, C2 domains: $cPLA_2C2$, PKCαC2, and Syt1C2A.

### *Intracellular Targeting of $cPLA_2C2$ Domain*

We have previously shown that FP fusions of $cPLA_2$ (FP-$cPLA_2$) and the $cPLA_2C2$ domain (FP-$cPLA_2C2$) colocalize completely after $Ca^{2+}$-mediated translocation, demonstrating that the C2 domain is entirely responsible for targeting of the enzyme. We have also demonstrated previously that FP-$cPLA_2$ colocalizes with golgin 97, a *cis*-Golgi cisternae marker and that FP-$cPLA_2C2$ colocalizes with ECFP-GT, which is a marker for medial and *trans*-Golgi cisternae, but not TGN (Sciaky *et al.*, 1997; Evans *et al.*, 2001, 2003). To better define $cPLA_2$ targeting, we compared colocalization of FP-$cPLA_2C2$ with FP-TGN38, a TGN marker (Keller *et al.*, 2001), and with FP-GT. MDCK cells coexpressing FP-$cPLA_2C2$ and FP-GT were stimulated with 10 μM ionomycin (IONO) and imaged by time-lapse microscopy. Images demonstrate colocalization of FP-$cPLA_2C2$ with FP-GT at Golgi (Figure 2A-C and Fig 2Cvideo) and at ER and nuclear membranes. These images also show dynamic, nuclear invaginations looking like intranuclear tubules to which $cPLA_2C2$ translocates (Ellenberg *et al.*, 1997; Fricker *et al.*, 1997; Evans *et al.*, 2001). To determine if Golgi cisternae could be differentiated from TGN, MDCK cells coexpressing FP-GT and FP-TGN38 were imaged. The FP-GT and FP-TGN38 signals were juxtaposed, but displayed little overlap (Figure 2D-F and Fig 2Fvideo). Most overlap was observed near the nucleus, where the cell is thickest, suggesting that the fluorescence overlap may be due to superpositioning of Golgi cisternae and TGN instead of colocalization of the markers on the same membranes. We would expect, based on these observations, that $cPLA_2C2$ targeting to be distinct from TGN. In IONO-treated MDCK cells coexpressing FP-$cPLA_2C2$ and FP-TGN38, the FP-$cPLA_2C2$ and FP-TGN38 signals were juxtaposed in a manner similar to TGN38 and GT (Figure 2, G–I), but failed to overlap well except very near the nucleus. These results demonstrate that the C2 domain of $cPLA_2$ preferentially targets ER and Golgi cisternae, although it is possible that a small fraction of $cPLA_2C2$ also localizes to the TGN.

### *Intracellular Targeting of PKCαC2 Domain*

Many reports have shown that PKCα and its C2 domain translocate to the plasma membrane in response to an $[Ca^{2+}]_i$ increase (Mineo *et al.*, 1998; Almholt *et al.*, 1999; Corbalán-García *et al.*, 1999; Maasch *et al.*, 2000; Bolsover *et al.*, 2003). Besides its C2 domain, PKCα also has a C1 domain that targets diacylglycerol in plasma membrane and can promote translocation of PKCα to plasma membrane in the absence of a $Ca^{2+}$ signal (Oancea and Meyer, 1998). Thus, it is possible that the C1 or other domains may modify $Ca^{2+}$- and C2 domain-dependent targeting of PKCα. To determine whether the PKCαC2 domain is solely responsible for $Ca^{2+}$-dependent membrane targeting, as is the case for $cPLA_2$, FP fusions of full-length PKCα and the isolated C2 domain were coexpressed in MDCK cells, stimulated with IONO, and imaged by time-lapse microscopy. In unstimulated cells, PKCα was primarily restricted to the cytoplasm, whereas the C2 domain was found also in the nucleoplasm (our unpublished data). PKCα (Figure 3A) and PKCαC2 (Figure 3B) rapidly moved from the cytoplasm to areas on the plasma membrane in response to IONO, where they overlapped completely (Figure 3C). This result demonstrates that the PKCαC2 domain is responsible for targeting of the holoenzyme in response to increases in $[Ca^{2+}]_i$. The distribution of PKCα and PKCαC2 on the plasma membrane was not uniform, but exhibited a punctate distribution on the dorsal cell surface (Figure 3D) and mottled appearance at

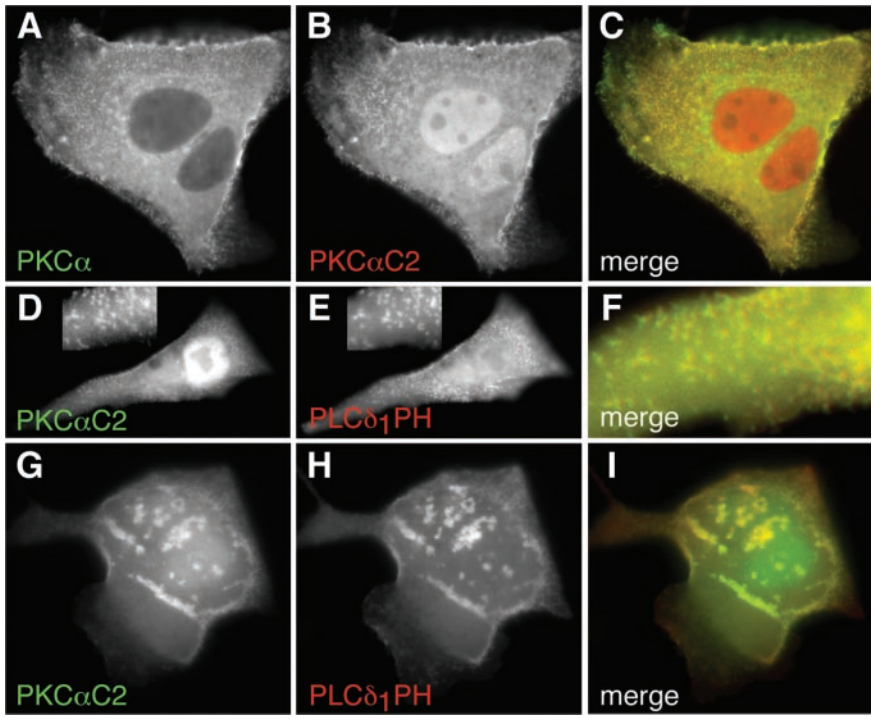


**Figure 3.** PKCα C2 domain is responsible for PKCα targeting and targets $PIP_2$-rich regions in the plasma membrane. Images of a cell coexpressing (A) ECFP-PKCα and (B) EYFP-PKCαC2 at 15 s after treatment with 10 μM IONO are shown. (C) A merged image of A and B. Images of a cell coexpressing (D) EYFP-PKCαC2 and (E) ECFP-PLCδ$_1$PH at 10 s after treatment with 10 μM IONO are shown. Focusing is on the dorsal surface of the cell. Insets in D and E show an enlarged area of the cell. A merged image (F) shows a smaller region of the cell. Images of a cell coexpressing (G) EYFP-PKCαC2 and (H) ECFP-PLCδ$_1$PH at 21 s after treatment with 10 μM IONO are shown. Focusing is on the ventral surface of the cell. A merged image (I) shows overlap of images G and H. Images are representative of a minimum of five experiments.

the ventral surface (Figure 3G and Fig 3Gvideo), similar to previous reports (Maasch *et al*., 2000) and similar to the reported distribution of the PLCδ$_1$PH domain (Stauffer *et al*., 1998; Varnai and Balla, 1998). Indeed, in response to IONO, FP-PKCαC2 (Figure 3, D and G) and FL-PLCδ$_1$PH fluorescence (Figure 3, E and H) overlapped at both the dorsal and ventral cell surfaces (Figure 3, F and I, respectively). However, unlike PKCαC2, PLCδ$_1$PH loses its punctate and irregular distribution within tens of seconds as the $[Ca^{2+}]_i$ increases and becomes homogeneous in the cytosol (Fig 3Hvideo), as has been described previously (Varnai and Balla, 1998). Because PLCδ$_1$PH specifically recognizes phosphatidylinositol-4,5-bisphosphate ($PIP_2$) in plasma membranes (Stauffer *et al*., 1998; Varnai and Balla, 1998; Balla and Varnai, 2002), these results suggest that PKCαC2 specifically targets areas in the plasma membrane enriched in $PIP_2$, consistent with observations that the PKCαC2 prefers anionic membrane phospholipids (Corbalán-García *et al*., 1999; Verdaguer *et al*., 1999; Kohout *et al*., 2002; Ochoa *et al*., 2002) and that the β 3 and 4 strands of PKCαC2 are involved in specific binding of $PIP_2$ (Corbalán-García *et al*., 2003).

### *Intracellular Targeting of PKCαC2 Mutants*

The tips of CBLs 1 and 3 of cPLA$_2$C2 contain hydrophobic residues that insert into the hydrophobic core of the membrane bilayer. In particular, F35 on loop 1 and Y96 on loop 3 have been shown to penetrate well into the membrane (Nalefski and Falke, 1998; Perisic *et al*., 1998, 19999; Bittova *et al*., 1999; Frazier *et al*., 2002; Stahelin *et al*., 2003). To deter-

**Table 1.** The calculated electrostatic free energy of interaction ($\Delta G_{el}$) of $Ca^{2+}$-bound C2 domains with a membrane containing 33 mole percent acidic lipid in 0.1 M KCl. See MATERIALS AND METHODS for details.

| C2 domain | ($\Delta G_{el}$), kcal/mol |
|---|---|
| PKCαC2 | −4.5 |
| Syt1C2A | −5.6 |
| cPLA$_2$C2 | +0.6 |
| Syt1C2A_cPLA$_2$C2_L1.2.3 | 0.0 |
| PKCαC2_cPLA$_2$C2_L1.2.3 | −0.5 |

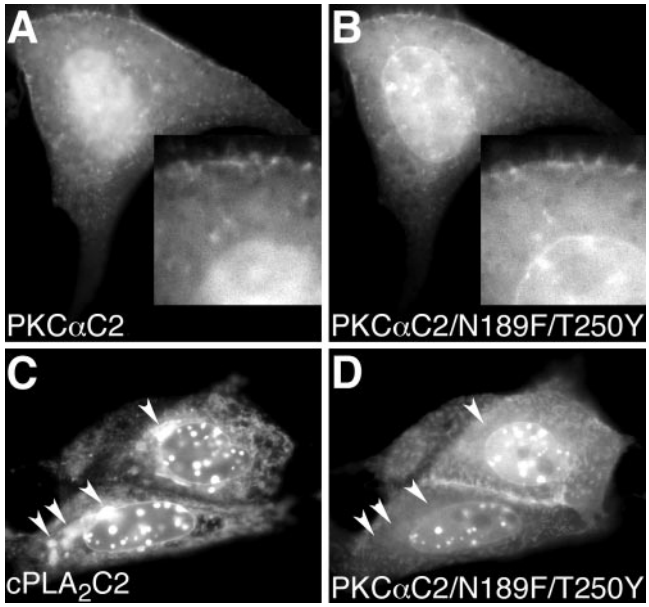


**Figure 4.** PKCαC2 domains containing hydrophobic residues target plasma and nuclear membranes, but not Golgi and ER. Images of a cell coexpressing (A) EYFP-PKCαC2 and (B) ECFP-PKCαC2/N189F/T250Y at 150 s after treatment with 10 μM IONO are shown. Insets in A and B show an enlarged area of the cell, including the nuclear membrane. Images of a cell coexpressing (C) EYFP-cPLA$_2$C2 and (D) ECFP-PKCαC2/N189F/T250Y at 240 s after treatment with 10 μM IONO are shown. Arrowheads in C point to Golgi and, in D, to the same area as in C. Images are representative of at least five experiments performed on different days.

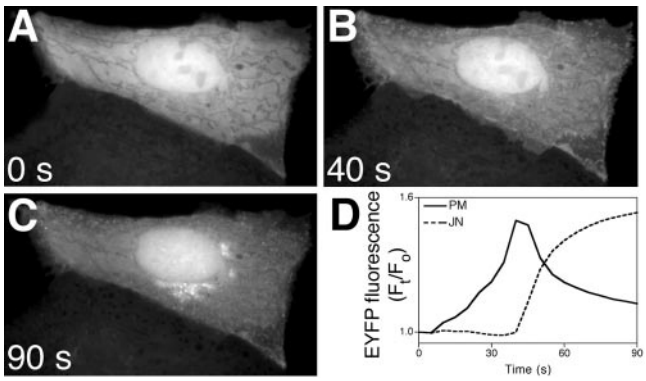


**Figure 5.** The Syt1C2A domain exhibits a biphasic pattern of translocation. Images of a cell expressing EYFP-Syt1C2A in medium supplemented with 5 mM $CaCl_2$ treated with 10 $\mu$M IONO show distribution of Syt1C2A (A) before, (B) 40 s and (C) 90 s after addition of IONO. (D) Quantification of fluorescence change at areas corresponding to the plasma membrane (PM, solid line) and the juxtanuclear (JN, dotted line) regions of the cell in images A–C. Images and graph are representative of six independent experiments.

mine whether addition of hydrophobic residues on PKC$\alpha$C2 would result in ER/Golgi targeting, a FP-PKC$\alpha$C2/N189F/T250Y mutant was constructed and coexpressed in cells with FP-PKC$\alpha$C2. PKC$\alpha$C2 N189 is located at the tip of CBL1, and PKC$\alpha$C2 T250 is located at a structurally similar site as $cPLA_2$C2 Y96, both in CBL3. FP-PKC$\alpha$C2/N189F/T250Y (Figure 4B) targeted plasma membrane, as did FP-PKC$\alpha$C2 (Figure 4A); however, the mutant also targeted nuclear membrane, unlike the wild-type PKC$\alpha$C2 domain. As seen in Figure 4C and in previous work, $cPLA_2$C2 targets Golgi (arrowheads), ER, and nuclear membrane, including the nuclear membrane invaginations. In cells coexpressing FP-PKC$\alpha$C2/N189F/T250Y and FP-$cPLA_2$C2 and treated with IONO, the mutant was observed at plasma membrane and colocalized with FP-$cPLA_2$C2 on the nuclear membrane and its invaginations, but it failed to colocalize at the ER or Golgi (Figure 4, C and D, arrowheads, and Fig 4Dvideo). Similar results were obtained with FP-PKC$\alpha$C2/N189F (our unpublished data). Comparison of the electrostatic profile models of PKC$\alpha$C2 and PKC$\alpha$C2/N189F/T250Y (Figure 10, A and D, respectively) show that they are very similar. Therefore, if electrostatic determinants are important in membrane targeting, then PKC$\alpha$C2 and PKC$\alpha$C2/N189F/T250Y would exhibit similar targeting. Together, these results demonstrate that adding hydrophobic residues to PKC$\alpha$C2 adds the nuclear membrane to its targeting pattern but fails to confer ER/Golgi targeting similar to $cPLA_2$C2 or change the electrostatic profile.

### *Intracellular Targeting of Syt1C2A Domain*

Although Syt1 is an integral membrane protein and its C2A domain mediates membrane binding but not translocation (Davletov and Sudhof, 1993; Chapman and Jahn, 1994; Geppert *et al*., 1994; Sudhof and Rizo, 1996; Zhang *et al*., 1998), analyzing its intracellular targeting pattern can help to reveal the properties of C2 domains that confer intracellular targeting. MDCK cells expressing FP fused to Syt1C2A (FP-Syt1C2A) were treated with IONO and imaged by time-lapse microscopy. In contrast to $cPLA_2$C2 and PKC$\alpha$C2, translocation of Syt1C2A required that the medium be supplemented with 5 mM $CaCl_2$ (final extracellular calcium ($[Ca^{2+}]_e$) = 6.3 mM), which reflects the lower affinity of Syt1C2A for $Ca^{2+}$ relative to $cPLA_2$C2 and PKC$\alpha$C2 (Nalefski and Newton, 2001; Kohout *et al*., 2002). In unstimulated MDCK cells, FP-Syt1C2A is distributed homogeneously in the cytoplasm and nucleoplasm. In response to IONO, FP-Syt1C2A exhibited a biphasic targeting pattern and first targeted the plasma membrane region in a similar pattern to FP-PKC$\alpha$C2 (Figure 5, A and B, and Fig 5video). However, unlike FP-PKC$\alpha$C2, FP-Syt1C2A partially dissociated from plasma membrane and moved to a juxtanuclear region several seconds after IONO treatment (Figure 5C and Fig 5video). Quantitative analysis of FP-Syt1C2A translocation (Figure 5D) shows the biphasic nature of Syt1C2A targeting. Although the timing varied between experiments, the pattern of FP-Syt1C2A first moving to the plasma membrane and then to the juxtanuclear area was consistently observed. To identify specific membrane domains and organelles targeted by FP-Syt1C2A, experiments similar to those described above were performed. Cells coexpressing FP-Syt1C2A and FP-PLC$\delta_1$PH were treated with IONO and imaged by time-lapse microscopy. The distribution of FP-PLC$\delta_1$PH looks punctate and irregular, as noted previously (Figure 6A). In the earliest times of FP-Syt1C2A translocation (9 s; Figure 6B), there is a partial overlap of the FP-PLC$\delta_1$PH and FP-Syt1C2A signals at the margins of the cell (Figure 6C). These results suggest that, initially, FP-Syt1C2A specifically targets areas of plasma membrane enriched in $PIP_2$ in a manner similar to FP-PKC$\alpha$C2. It was not possible to image colocalization of FP-PLC$\delta_1$PH and FP-Syt1C2A at later times due to rapid dissociation of FP-PLC$\delta_1$PH from the plasma membrane. Because the juxtanuclear targeting of FP-Syt1C2A seen later is reminiscent of Golgi cisternae or TGN (Figure 2), probes were used to identify the structure targeted in the later phase of Syt1C2A translocation. The majority of the FP-TGN38 fluorescence in the cell is located in a juxtanuclear position representing TGN; however, there was a small fraction of fluorescence located at small, motile structures, presumably endosomes, and at the plasma membrane (Figure 6D). After IONO treatment, FP-Syt1C2A (Figure 6E) overlapped with the TGN fraction of the FP-TGN38 fluorescence, but not with the endosomal or plasma membrane fractions (Figure 6F). Conversely, when FP-Syt1C2A was coimaged with FP-GT (Figure 6, H and G, respectively), or with FP-Rab5 (Figure 6, K and J, respectively), a marker for early endosomes (Novick and Zerial, 1997), there was only a small region of overlap of the fluorescence (Figure 6, I and L). The spatial relationship between FP-Syt1C2A and FP-Rab5 (Figure 6L) was similar to that between FP-Syt1C2A and the endosomes identified by FP-TGN38 (Figure 6F). Similar experiments using FP-Rab8, a marker for late endosomes, showed no overlap of fluorescence with Syt1C2A (our unpublished data). TGN was further identified as the site of Syt1C2A translocation by coimaging cells expressing FP-$cPLA_2$C2 and FP-Syt1C2A in response to $[Ca^{2+}]_i$ mobilization after incubation for 1.5 h in 100 $\mu$M brefeldin A (BFA), which disrupts Golgi cisternae but not TGN (Lippincott-Schwartz *et al*., 1989; Chege and Pfeffer, 1990). In response to an increase in $[Ca^{2+}]_i$, no clear $cPLA_2$C2 targeting of Golgi was observed (compare Figure 6M with Figures 3, 8, and 9), demonstrating that BFA had disrupted targeting to Golgi as we have shown previously (Evans *et al*., 2001). However, BFA had no effect on Syt1C2A translocation (Figure 6N). These results suggest that the TGN is the primary target of the later phase of Syt1C2A translocation.

The biochemical and electrostatic characteristics of Syt1C2A and PKC$\alpha$C2 membrane binding are very similar

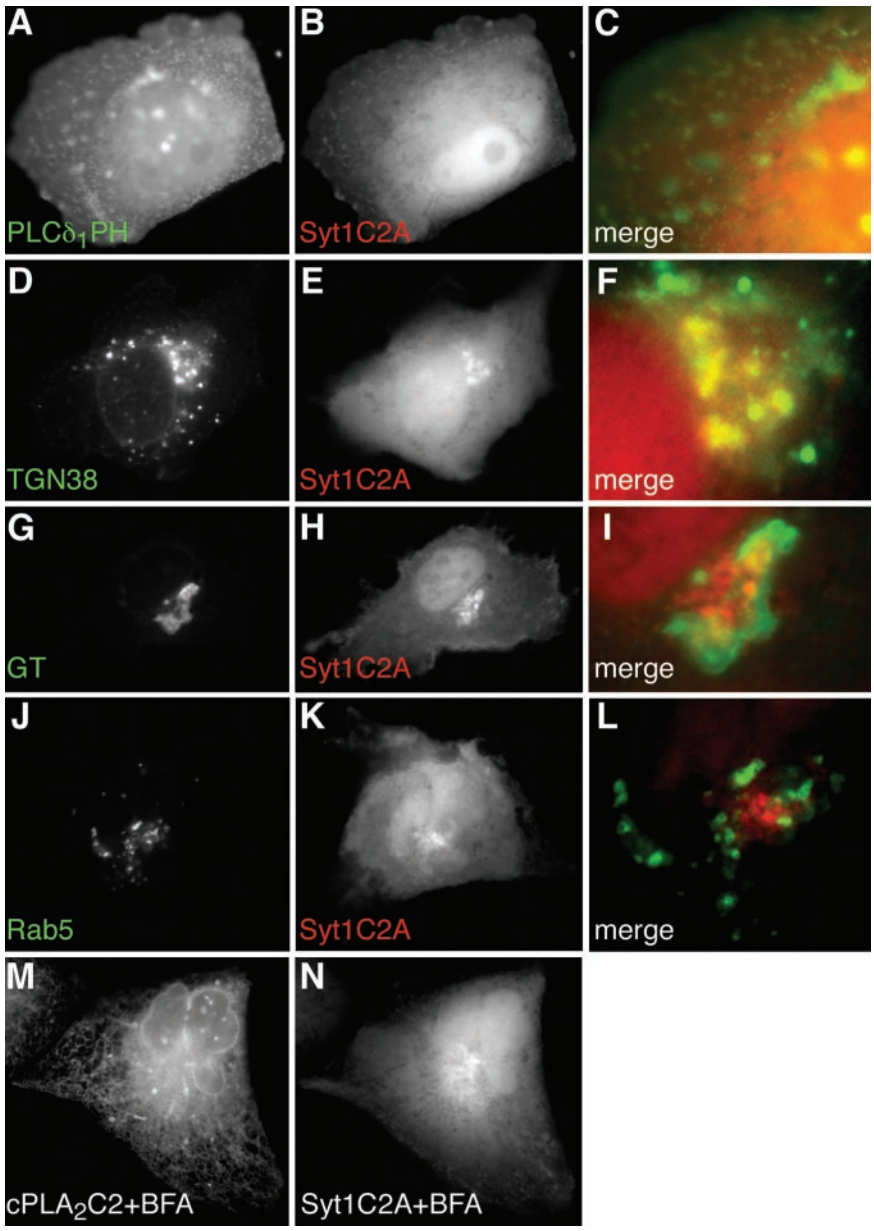


**Figure 6.** Syt1C2A targets TGN and $PIP_2$-rich regions in the plasma membrane. Images of a cell coexpressing (A) ECFP-PLC$\delta_1$PH and (B) EYFP-Syt1C2A in medium supplemented with 5 mM $CaCl_2$ at 9 s after treatment with 10 $\mu$M IONO are shown. A merged image (C) shows a region of the cell membrane. Images of a cell coexpressing (D) TGN38-ECFP and (E) EYFP-Syt1C2A in medium supplemented with 5 mM $CaCl_2$ at 56 s after treatment with 10 $\mu$M IONO are shown. A merged image (F) shows the region of the TGN. Images of a cell coexpressing (G) ECFP-GT and (H) EYFP-Syt1C2A in medium supplemented with 5 mM $CaCl_2$ at 20 s after treatment with 10 $\mu$M IONO are shown. A merged image (I) shows the region of TGN and Golgi. Images of a cell coexpressing (J) ECFP-Rab5 and (K) EYFP-Syt1C2A in medium supplemented with 5 mM $CaCl_2$ at 20 s after treatment with 10 $\mu$M IONO are shown. A merged image (L) shows the region of early endosomes and TGN. Cells coexpressing (M) ECFP-$cPLA_2C2$ and (N) EYFP-Syt1C2A were treated for 1.5 h with 100 $\mu$M BFA at 37°C before stimulation with 10 $\mu$M IONO in medium supplemented with 5 mM $CaCl_2$. Images are 20 s after stimulation. Images are representative of a minimum of five experiments.

(Nalefski *et al*., 2001; Kohout *et al*., 2002; Murray and Honig, 2002) and it was unexpected that the two C2 domains would exhibit different targeting profiles. Because Syt1C2A required increased $[Ca^{2+}]_e$ for translocation, we examined whether PKC$\alpha$C2 also targeted TGN and displayed a biphasic targeting pattern in response to an increased $[Ca^{2+}]_e$. Cells coexpressing FP-PKC$\alpha$C2 and FP-Syt1C2A were stimulated with IONO in medium supplemented with 5 mM $CaCl_2$ and imaged by time-lapse microscopy. No difference was observed between the targeting of PKC$\alpha$C2 in medium containing ~1.3 mM (Figure 3B) or ~6.3 mM (Figure 7A) $CaCl_2$. Thus, the difference between the targeting patterns of Syt1C2A and PKC$\alpha$C2 (Figure 7, A–C) is not an artifact of increased $[Ca^{2+}]_e$.

### *Intracellular Targeting of a Syt1C2A/cPLA$_2$C2 Hybrid C2 Domain*

Having established the targeting patterns of the individual C2 domains, we proceeded to investigate the importance of the $cPLA_2C2$ CBLs in determining intracellular targeting of $cPLA_2C2$. A FP fusion of a hybrid C2 domain consisting of $cPLA_2C2$ CBLs substituted into Syt1C2A was used (Figure 8, A and B) (Gerber *et al*., 2001). In liposome binding assays, the hybrid Syt1C2A/$cPLA_2C2$ domain displayed lipid specificity similar to $cPLA_2C2$ (Gerber *et al*., 2001). Because $cPLA_2C2$ and Syt1C2A display Golgi/ER and plasma membrane/TGN targeting, respectively, we expected to observe little similarity between the $Ca^{2+}$-dependent targeting patterns of $cPLA_2C2$ and Syt1C2A in the same cell. In response to IONO in medium supplemented with 5 mM $CaCl_2$, $cPLA_2C2$ displayed the usual targeting of ER, Golgi, and nuclear membrane (Figure 8C). In contrast, Syt1C2A was observed primarily at the TGN (Figure 8D). Consistent with our earlier observations, FP-$cPLA_2C2$ and FP-Syt1C2A fluorescence signals are primarily juxtaposed and only partial overlap in the area of the Golgi (Figure 8E). Of particular interest was the observation that Syt1C2A failed to target nuclear membrane invaginations or ER; in fact, FP-Syt1C2A fluorescence was

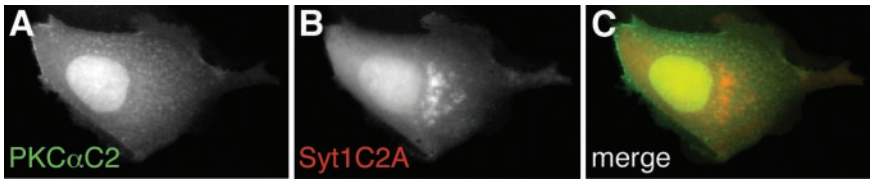


**Figure 7.** Syt1C2A and PKCαC2 target different subcellular organelles in response to a $[Ca^{2+}]_i$ increase. Cells coexpressing (A) ECFP-PKCαC2 and (B) EYFP-Syt1C2A in medium supplemented with 5 mM $CaCl_2$ at 55 s after treatment with 10 μM IONO are shown. (C) A merged image of A and B. Images are representative of a minimum of five experiments.

excluded from the area of the ER. In contrast, a FP-tagged, hybrid C2 domain containing CBLs1, 2, and 3 from $cPLA_2$ on a Syt1C2A backbone (Syt1C2A_$cPLA_2$C2_L1.2.3; Figure 8G and Fig 8Gvideo) displayed an intracellular targeting pattern that was indistinguishable from $cPLA_2$C2, although translocation of the hybrid required a higher (6.3 mM) $[Ca^{2+}]_e$. This Syt1C2A/$cPLA_2$C2 hybrid targeted Golgi, ER, and the nuclear membrane invaginations, but not plasma membrane or TGN. This result demonstrates that the CBL regions of $cPLA_2$C2 confer targeting to Golgi and ER and that substituting $cPLA_2$C2 CBLs results in a complete switch in the targeting pattern. However, this Syt1C2A/$cPLA_2$C2 hybrid domain also included portions of $cPLA_2$C2 β strands that are below the $Ca^{2+}$-binding regions (Figure 8, A and B), which may have influenced targeting.

### *Intracellular Targeting of PKCαC2/cPLA$_2$C2 Hybrid C2 Domains*

To investigate to role of specific $cPLA_2$C2 CBLs in more detail, FP-tagged PKCαC2/$cPLA_2$C2 hybrids were constructed that contained $cPLA_2$C2 CBLs 1, 2, and 3, or 1 and 3 on a PKCαC2 backbone. The CBLs in the PKCαC2/$cPLA_2$C2 hybrids contained fewer residues than the CBLs in the Syt1C2A/$cPLA_2$C2 hybrid (Figure 9, A and B). To verify the different targeting patterns of $cPLA_2$C2 and PKCαC2, cells coexpressing FP-$cPLA_2$C2 and FP-PKCαC2 were treated with IONO and imaged. FP-$cPLA_2$C2 (Figure 9A) and FP-PKCαC2 (Figure 9B) translocated to very different areas of the cell (Figure 9E), as observed above. In contrast to FP-PKCαC2 targeting, a PKCαC2/$cPLA_2$C2 hybrid construct containing all three $cPLA_2$C2 CBLs (PKCαC2_$cPLA_2$C2_L1.2.3; Figure 9G and Fig 9Gvideo) translocated to the Golgi, ER, and nuclear membrane, in a pattern similar to $cPLA_2$C2 (Figure 9, F and H). To narrow down further the structures required for Golgi/ER targeting, similar experiments were performed with a PKCαC2/$cPLA_2$C2 hybrid construct containing $cPLA_2$C2 CBLs 1 and 3 (PKCαC2_$cPLA_2$C2_L1.3; Figure 9J and Fig 9Jvideo). This construct was observed to translocate to Golgi in a pattern similar to $cPLA_2$C2 (Figure 9F). However, PKCαC2_$cPLA_2$C2_L1.3 required a higher $[Ca^{2+}]_e$ than PKCαC2 (6.3 mM) and was not observed at the ER or nuclear envelope (Figure 9K). Targeting was observed at ER and nuclear membrane, but only when cells were treated with extremely high $[Ca^{2+}]_e$ (>25 mM), which also caused vesiculation of the ER and blebbing at the plasma membrane (our unpublished data). We have shown previously that $cPLA_2$C2 translocates to Golgi at lower $[Ca^{2+}]_i$ than it does to ER and nuclear membrane (Evans *et al.*, 2001), thus the observation of preferential Golgi targeting of the PKCαC2_$cPLA_2$C2_L1.3 construct was not unexpected. Together, these results suggest that $cPLA_2$ CBLs 1 and 3 confer Golgi/ER targeting and that inclusion of CBL2 improves $Ca^{2+}$ binding properties of the hybrid.

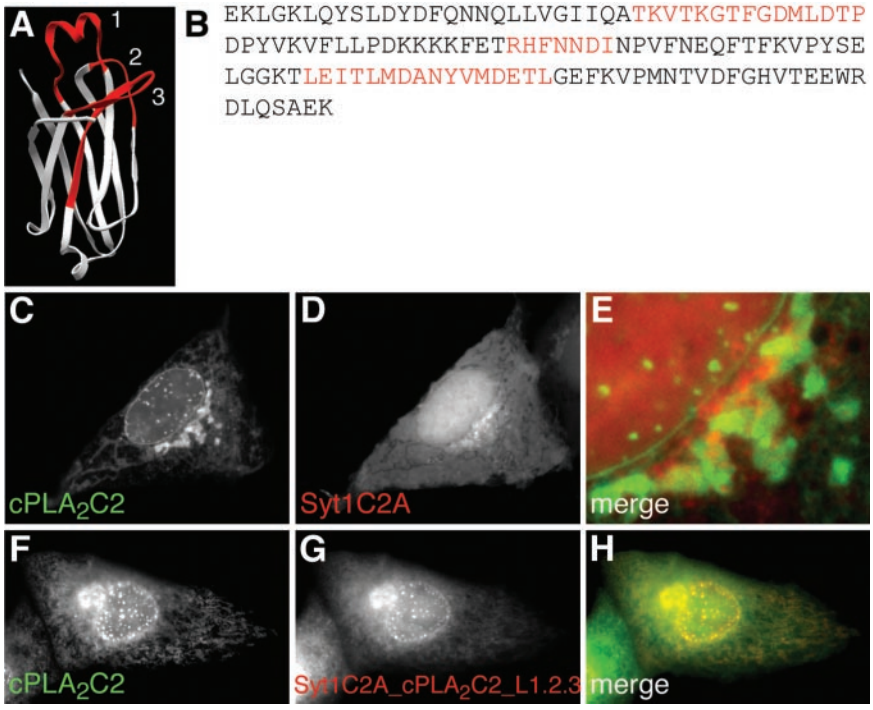


**Figure 8.** A hybrid Syt1C2A/$cPLA_2$C2 domain containing $cPLA_2$C2 $Ca^{2+}$-binding loops colocalizes with $cPLA_2$C2. (A) Ribbon diagram of the hybrid C2 domain with $Ca^{2+}$-binding loops from $cPLA_2$C2 (red) on a Syt1C2A backbone (white). (B) The amino acid sequence of the hybrid shows Syt1C2A sequence (black, E140-A165, D178-T195, N203-T223, G241-K267) interrupted by insertion of $cPLA_2$C2 loop sequences (red, T28-P42, R61-I67, L87-I102). Images of cells coexpressing ECFP-$cPLA_2$C2 (C) and EYFP-Syt1C2A (D) in medium supplemented with 5 mM $CaCl_2$ at 55 s after treatment with 10 μM IONO are shown. (E) A merged image of C and D. Images of cells coexpressing (F) EYFP-$cPLA_2$C2 and (G) ECFP-Syt1C2A_$cPLA_2$C2_L1.2.3 in medium supplemented with 5 mM $CaCl_2$ at 70 s after treatment with 10 μM IONO are shown. (H) A merged image of F and G.

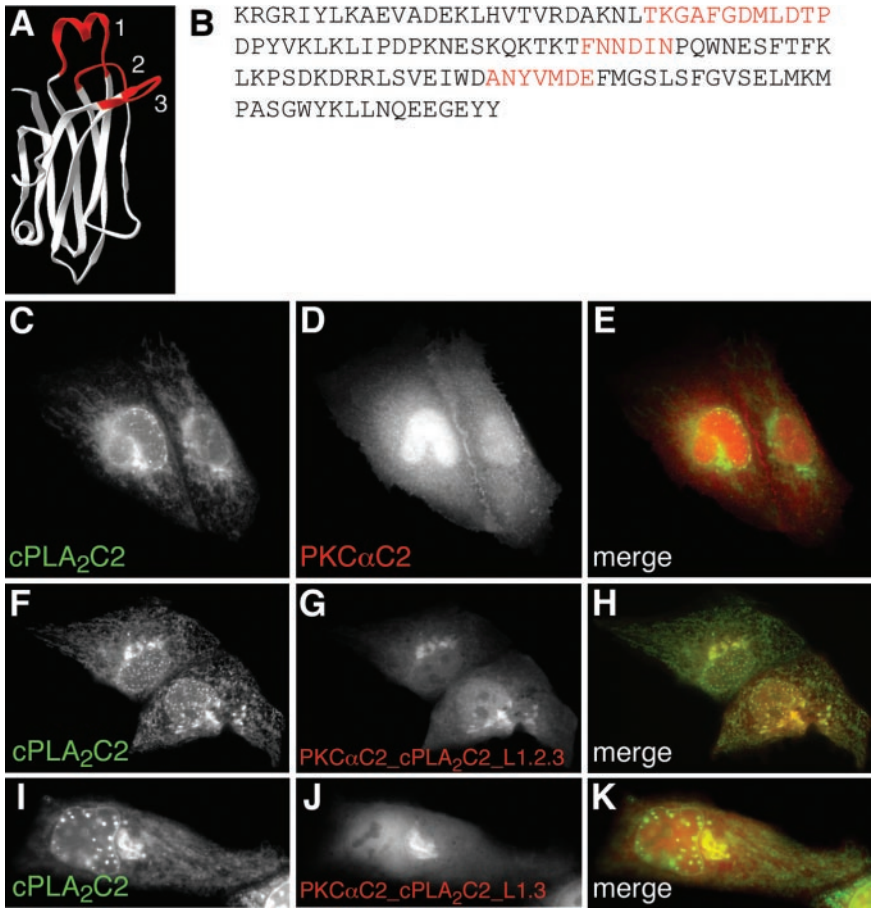


**Figure 9.** Hybrid PKC$\alpha$C2/cPLA$_2$C2 domains containing cPLA$_2$C2 $Ca^{2+}$-binding loops colocalize with cPLA$_2$C2. (A) Ribbon diagram of the hybrid C2 domain with $Ca^{2+}$-binding loops from cPLA$_2$C2 (red) on a PKC$\alpha$C2 backbone (white). (B) The amino acid sequence of the hybrid shows PKC$\alpha$C2 sequence (black, K158-L183, D193-T214, P221-D246, F255-Y285) interrupted by insertion of cPLA$_2$C2 loop sequences (red, T31-P42, F63-I67, A94-E100). Images of cells coexpressing (C) ECFP-cPLA$_2$C2 and (D) EYFP-PKC$\alpha$C2 at 45 s after treatment with 10 $\mu$M IONO are shown. (E) A merged image of C and D. Images of cells coexpressing (F) EYFP-cPLA$_2$C2 and (G) ECFP-PKC$\alpha$C2_cPLA$_2$C2_L1.2.3 at 90 s after treatment with 10 $\mu$M IONO are shown. (H) A merged image shows the overlap of F and G. Images of cells coexpressing (I) EYFP-cPLA$_2$C2 and (J) ECFP-PKC$\alpha$C2_cPLA$_2$C2_L1.3 in medium supplemented with 5 mM $CaCl_2$ at 42 s after treatment 10 $\mu$M IONO are shown. (K) A merged image shows the overlap of I and J.

### *Electrostatic $Ca^{2+}$ Binding of Syt1C2A/cPLA$_2$C2 and PKC$\alpha$C2/cPLA$_2$C2 Hybrids*

A recent computational study of the association of C2 domains with phospholipid membranes by using the FDPB method provides insight into the physical basis of C2 domain/membrane interactions. For example, the electrostatic free energy of interaction of $Ca^{2+}$-bound Syt1C2A with a membrane containing 33 mol% acidic lipid (2:1 PC/PS) was predicted to be −5.6 kcal/mol and highly dependent on ionic strength of the solution (Table 1, Figure 10B), which is in good agreement with experimental measurements (Gerber *et al*., 2001; Zhang *et al*., 1998; Nalefski *et al*., 2001) and suggest that electrostatic interactions are sufficient to mediate significant membrane binding. However, $Ca^{2+}$-bound cPLA$_2$C2, in a similar orientation, is predicated to have a positive electrostatic free energy of interaction (+0.6 kcal/mol) with 2:1 PC/PS due to electrostatic repulsions (Table 1, + 0.6 kcal, Figure 10C). The favorable electrostatic free energy of interaction for $Ca^{2+}$-bound Syt1C2A contrasts greatly with the unfavorable electrostatic free energy for $Ca^{2+}$-bound cPLA$_2$C2 at the membrane surface and highlights the mechanistic differences between Syt1C2A (primarily favorable electrostatic) and cPLA$_2$C2 (primarily hydrophobic) interactions with membrane. To determine the electrostatic contribution to the membrane association of other C2 domains considered in this study, FDPB calculations were performed with molecular models for PKC$\alpha$C2 and the hybrid C2 domains, and a 2:1 PC/PS membrane in 0.1 M KCl (Table 1, Figures 10A, 10E, and 10F). The electrostatic free energy of membrane interaction for $Ca^{2+}$-bound PKC$\alpha$C2 was −4.5 kcal/mol, which is similar to that of $Ca^{2+}$-bound Syt1C2A (−5.6 kcal/mol) (Murray and Honig, 2002). In contrast, the electrostatic free energies of membrane interaction for the PKC$\alpha$C2/cPLA$_2$C2 and Syt1C2A/cPLA$_2$C2 hybrids containing all three CBLs were −0.5 and 0.0 kcal/mol, respectively, and reminiscent of the repulsive electrostatic interactions experienced by cPLA$_2$C2. Thus, unlike Syt1C2A or PKC$\alpha$C2, but similar to cPLA$_2$C2, the contribution of electrostatic attraction to membrane binding for the hybrids is negligible and membrane binding is most probably due to hydrophobic interactions (Table 1).

## DISCUSSION

By comparing the spatiotemporal patterns of translocation between wild-type and mutant or hybrid C2 domains, we were able to correlate structural features of the cPLA$_2$C2 domain with $Ca^{2+}$-dependent targeting to Golgi and ER. Interestingly, topological differences between the cPLA$_2$C2 and Syt1C2A or PKC$\alpha$C2 domains were found to be relatively unimportant, because we were able to freely exchange homologous structures between types I (Syt1C2A and PKC$\alpha$C2) and II (cPLA$_2$C2) C2 domains. The coimaging approach used here allowed us to directly compare translocation of any two domains under identical conditions in a physiological setting, thus providing "built-in" controls for cell-to-cell heterogeneity in organelle morphology and in the amplitude and kinetics of the $[Ca^{2+}]_i$ increases. The dual imaging approach also allowed us to readily visualize subtle or gross changes in targeting of mutant and hybrid domains.

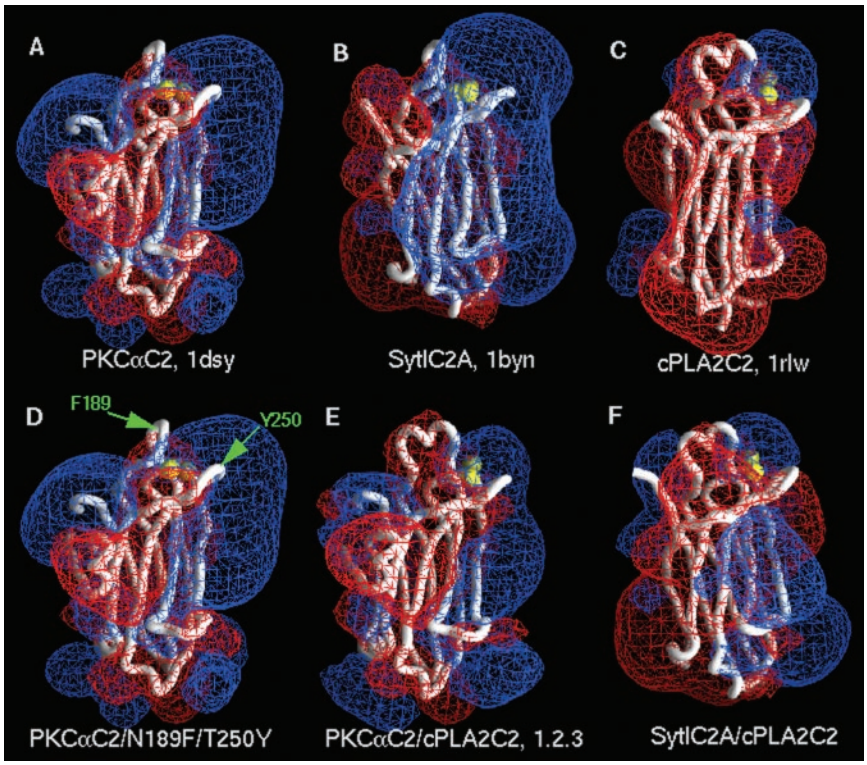


**Figure 10.** Electrostatic properties of C2 domains of known structure, mutants, and hybrid models. In each panel, the structure or model is represented as a Cα backbone worm (white), and calcium ions are represented as yellow spheres. The electrostatic potentials were calculated and visualized in GRASP (Nicholls et al., 1991) for 0.1 M KCl. The red and blue meshes represent, respectively, the −25 and +25 mV equipotential profiles. (A) PKCαC2. (B) Syt1C2A. (C) $cPLA_2C2$. (D) PKCαC2/N189F/T250Y; F189 and Y250 are denoted by green arrows. (E) PKCαC2_$cPLA_2$C2_L1.2.3. (F) Syt1C2A_$cPLA_2$ C2_L1.2.3. The structures in A, B, and C were taken from the Protein Data Bank, and the hybrid models in D, E, and F were constructed as described in MATERIALS AND METHODS.

### *Targeting of C2 Domains to the Plasma Membrane*

The inner leaflet of the plasma membrane serves as a platform on which a multitude of signaling complexes form in response to different cellular signals, including increases in $[Ca^{2+}]_i$. We demonstrate here that the C2 domain specifically targets PKCα to regions of the plasma membrane enriched in $PIP_2$, which is consistent with recent reports that lysine residues in the β3 and 4 strands of PKCαC2 specifically bind $PIP_2$ in vitro (Corbalán-García *et al.*, 2003). A primary role for the β 3–4 strand region in targeting, however, is questionable, because although PKCαC2/$cPLA_2$C2 hybrid domains have intact PKCαC2 β 3–4 strands, they fail to target $PIP_2$-rich areas of the plasma membrane. Because many reports have shown that specific binding of PKCαC2 to PS is important in membrane interaction (Verdaguer *et al.*, 1999; Conesa-Zamora *et al.*, 2001; Ochoa *et al.*, 2002), further work will be required to differentiate between the roles of nonspecific electrostatics and specific interactions between PKCαC2 and inner leaflet PS or $PIP_2$ in membrane targeting.

In contrast to the PKCαC2 domain, the Syt1C2A domain serves to facilitate the fusion of vesicles with plasma membrane in response to $[Ca^{2+}]_i$ signals. The observation here that the isolated Syt1C2A localizes to regions rich in $PIP_2$ in the plasma membrane is consistent with observations that Syt1C2A binds to liposomes containing $PIP_2$ and nonspecifically binds membranes containing anionic phospholipids (Zhang *et al.*, 1998; Murray and Honig, 2002). On the other hand, our finding that Syt1C2A exhibits a biphasic spatiotemporal targeting pattern and that the secondary target is the TGN, but not closely related membrane domains, suggests membrane-specific determinants, either lipid or protein, aid in Syt1C2A-membrane binding. It is possible that targeting of TGN is due to protein–protein interactions (Chapman *et al.*, 1995; Shao *et al.*, 1997; Sugita and Sudhof, 2000). For example, Syt1C2A binds to the N-terminal region of syntaxin 1a in a $Ca^{2+}$-dependent manner (Chapman *et al.*, 1995; Shao *et al.*, 1997) and syntaxin 6, which exhibits homology to the N-terminal region of syntaxin 1a (Misura *et al.*, 2002), is found at the TGN (Bock *et al.*, 1997). Alternatively, Syt1C2A targeting to TGN may involve a more complex interplay of specific phospholipid interaction, electrostatics, and hydrophobic forces. For example, phosphatidylinositol-4-phosphate has been identified as a constituent of the TGN in MDCK cells by using the phosphatidylinositol-4-phosphate adaptor protein 1 PH domain as a probe (Evans, unpublished observations; Dowler *et al.*, 2000; Balla and Varnai, 2002), and, although Syt1C2A association with membrane is primarily electrostatic in nature, several reports have demonstrated that CBL 3 of Syt1C2A can penetrate into the lipid core of membranes, although not as deeply as $cPLA_2$ (Chae *et al.*, 1998; Chapman and Davis, 1998; Frazier *et al.*, 2003). Perhaps both electrostatic and hydrophobic forces regulate Syt1C2A interaction with membrane. Given the biochemical and electrostatic similarities between PKCαC2 and Syt1C2A, it was surprising to observe the difference in targeting patterns, which may represent a fundamental difference between the modes of membrane interaction between these domains.

### *Targeting C2 Domains to Golgi and ER*

Of those C2 domains whose intracellular targeting in response to $[Ca^{2+}]_i$ signals has been studied, the $cPLA_2$C2 domain is unique in that it targets intracellular membranes exclusively. This is not entirely unexpected, because targeting ER and nuclear membranes may promote coupling of $cPLA_2$ to cyclooxygenases and 5-lipoxygenase, enzymes that metabolize AA produced by $cPLA_2$ that are located at ER and nuclear membranes, respectively (Funk, 2001).

Targeting of $cPLA_2$ to Golgi, ER, and nuclear membranes is very specific. We have reported previously that $cPLA_2$ translocation to Golgi is sensitive to BFA treatment, translocation is seen at Golgi "ministacks" in response to nocoda-

zole treatment and that cPLA$_2$ colocalizes with golgin 97, a *cis*-Golgi marker and with GT, a medial- and *trans*-Golgi marker (Evans *et al*., 2001, 2003). We have extended these observations to report here that cPLA$_2$C2 fails to colocalize substantially with TGN (Figure 2, D–I). The juxtaposed localization of TGN38 to cPLA$_2$C2 was very similar to the localization of TGN38 to GalNAc transferase II, a Golgi cisternae marker, in PtK$_2$ cells (Keller *et al*., 2001). If cPLA$_2$ targeting requires specific protein or lipid determinants, it is possible that those determinants are not present in TGN membranes.

The observation that the Syt1C2A/cPLA$_2$C2 hybrid faithfully recapitulates cPLA$_2$C2 targeting points to the important role of the CBLs in Golgi/ER targeting. The higher $[Ca^{2+}]_e$ required for hybrid translocation, compared with cPLA$_2$C2, is consistent with the significantly lower $Ca^{2+}$ affinity of the Syt1C2A/cPLA$_2$C2 hybrid compared with cPLA$_2$C2 in binding to liposomes, probably due to incorrect geometry of the $Ca^{2+}$-coordinating residues (Gerber *et al*., 2001). The PKC$\alpha$C2 domain was chosen for making the hybrids because, like cPLA$_2$C2, it binds two $Ca^{2+}$ ions and has significant homology to cPLA$_2$C2 in the core region. These hybrids contained swapped loops that were two to nine residues smaller than similar swaps in the Syt1C2A/cPLA$_2$C2 hybrid (Figures 7B and 8B). A PKC$\alpha$C2/cPLA$_2$C2 hybrid with only a swapped CBL1 remained cytoplasmic even when the $[Ca^{2+}]_e$ was raised to very high levels (our unpublished data), possibly due to an inability to bind $Ca^{2+}$, as was the case for Syt1C2A/cPLA$_2$C2 hybrids containing only CBL3 or CBLs1 and 2 (Gerber *et al*., 2001). However, addition of cPLA$_2$C2 CBLs 1 and 3 to PKC$\alpha$C2 resulted in Golgi targeting, but also required a higher $[Ca^{2+}]_e$. This lower affinity for $Ca^{2+}$ of the CBL 1.3 hybrid is probably due to the lack of the $Ca^{2+}$ coordinating residue, N65, located in CBL2 of cPLA$_2$C2 (Perisic *et al*., 1998; Xu *et al*., 1998). The CBL 1.3 hybrid could be driven to ER at high $[Ca^{2+}]_e$, consistent with our results that demonstrated that cPLA$_2$C2 preferentially translocates to Golgi at lower $[Ca^{2+}]_i$ (Evans *et al*., 2001). The CBL 1.2.3 hybrid translocated to Golgi and ER without increasing the $[Ca^{2+}]_e$, again suggesting that CBL 2 is important for $[Ca^{2+}]_i$ binding, but is not involved in targeting Golgi and ER membranes. These results suggest that the CBLs are sufficient for Golgi/ER targeting. A reciprocal hybrid C2 domain, where the PKC$\alpha$C2 CBLs are fused to a cPLA$_2$C2 backbone, fails to target Golgi/ER, demonstrating that the cPLA$_2$C2 CBLs are both necessary and sufficient and that there are no other Golgi/ER targeting determinants on the rest of the cPLA$_2$C2 domain (Evans, unpublished observations). Similarly, we showed that simply substituting hydrophobic residues at the tips of PKC$\alpha$C2 CBLs 1 and 3 fails to change the targeting pattern of PKC$\alpha$ to one resembling cPLA$_2$C2.

The electrostatic equipotential profiles qualitatively demonstrate that the binding of $Ca^{2+}$ to PKC$\alpha$C2 and Syt1C2A relies on electrostatic forces, and the FDPB calculations show that the electrostatic free energy of interaction favors electrostatic interaction of PKC$\alpha$C2 and Syt1C2A with membranes containing anionic lipids (Murray and Honig, 2002). This contrasts greatly with the FDPB results obtained for cPLA$_2$C2 and the Syt1C2A/cPLA$_2$C2 and PKC$\alpha$C2/cPLA$_2$C2 hybrids, which show that electrostatic free energy of interaction between these domains and membrane was unfavorable in all conditions simulated (Murray and Honig, 2002). Thus, binding of cPLA$_2$C2 and the hybrid C2 domains to membrane most likely relies on hydrophobic interactions facilitated by the binding of $Ca^{2+}$, which reduces the free energy of interaction as a function of membrane penetration by neutralizing the negatively charged $Ca^{2+}$-binding residues (Figure 10C), thus allowing membrane penetration.

The results of this study contribute to the understanding of the structural elements and electrostatic changes required for targeting to Golgi and ER membranes. It has been suggested that translocation of cPLA$_2$C2 to interior membranes is due to the distribution of PC (Stahelin *et al*., 2003). However, a study on lipid content in different membrane compartments in CHO cells has shown that PC is equally abundant, as a percentage of total phospholipids, in Golgi and plasma membrane (Gkantiragas *et al*., 2001). We find that targeting of cPLA$_2$C2 in Chinese hamster ovary cells is identical to that observed in MDCK cells (Evans, unpublished observations). These observations suggest that other factors in these membranes may play a role in cPLA$_2$C2 targeting, which is supported by the observations that the $[Ca^{2+}]_i$ required for cPLA$_2$C2 membrane association in live cells is an order of magnitude lower than what has been reported for binding to PC vesicles in vitro. Previous reports have suggested that PIP$_2$ plays a role in activation of cPLA$_2$ (Leslie and Channon, 1990; Mosior *et al*., 1998), and a recent report suggests that residues in the cPLA$_2$ catalytic domain bind PIP$_2$ (Six and Dennis, 2003). In our results here, however, we find no evidence for the C2 domain targeting areas rich PIP$_2$ as determined by FP-tagged PLC$\delta_1$PH domain localization. However, a high-resolution study with glutathione *S*-transferase-tagged PLC$\delta_1$PH domain has demonstrated only a small fraction of PIP$_2$ at the Golgi stacks and ER (Watt *et al*., 2002), suggesting that small amounts of PIP$_2$ may have a role in cPLA$_2$ activation, but not targeting. Ceramide, a constituent of the Golgi, has been shown to bind the cPLA$_2$ C2 domain and increase the fraction of cPLA$_2$ bound to membrane in response to an increase in $Ca^{2+}$, possibly by modifying the phospholipid organization in membranes (Sato *et al*., 1999; Kitatani *et al*., 2000; Huwiler *et al*., 2001). Several proteins have been shown to interact with cPLA$_2$C2 in vitro, including annexins (Buckland and Wilton, 1998; Solito *et al*., 1998), vimentin (Nakatani *et al*., 2000), and PLIP (Sheridan *et al*., 2001), but it is not clear as to their role in targeting. Further investigation will aim to identify the lipid or protein constituents of Golgi that aid in cPLA$_2$ targeting.

Besides its role in generation of AA, an intriguing role for cPLA$_2$ may be in membrane remodeling that is important for membrane trafficking. Many recent studies have implicated PLA$_2$ activity in constitutive membrane trafficking (Choukroun *et al*., 2000; Brown *et al*., 2003). Most reports, however, implicate calcium-independent PLA$_2$ isoforms and because cPLA$_2$ is only on membranes after an increase in $[Ca^{2+}]_i$, it would not be a good candidate for regulating constitutive trafficking. On the other hand, cPLA$_2$ may play a role in trafficking in response to $[Ca^{2+}]_i$ signals, although there have been no studies investigating this possibility.

## ACKNOWLEDGMENTS

This work was supported by National Institutes of Health grants HL-61378 and HL-34303 (to C.C.L.), an Individual National Research Service Award (HL10507), and an Aronsen Fellowship from National Jewish Medical and Research Center (to J.H.E.), and National Institutes of Health grant GM-66147 (to D.M.).

## REFERENCES

Almholt, K., Arkhammar, P.O., Thastrup, O., and Tullin, S. (1999). Simultaneous visualization of the translocation of protein kinase C alpha-green fluorescent protein hybrids and intracellular calcium concentrations. Biochem. J. *337*, 211–218.

Arcaro, A., Volinia, S., Zvelebil, M.J., Stein, R., Watton, S.J., Layton, M.J., Gout, I., Ahmadi, K., Downward, J., and Waterfield, M.D. (1998). Human phosphoinositide 3-kinase C2 beta, the role of calcium and the C2 domain in enzyme activity. J. Biol. Chem. *273*, 33082–33090.

Balla, T., and Varnai, P. (2002). Visualizing cellular phosphoinositide pools with GFP-fused protein-modules. Science's Stke: signal transduction knowledge environment. PL3.

Ben-Tal, N., Honig, B., Miller, C., and McLaughlin, S. (1997). Electrostatic binding of proteins to membranes. Theoretical predictions and experimental results with charybdotoxin and phospholipid vesicles. Biophys. J. *73*, 1717–1727.

Ben-Tal, N., Honig, B., Peitzsch, R.M., Denisov, G., and McLaughlin, S. (1996). Binding of small basic peptides to membranes containing acidic lipids: theoretical models and experimental results. Biophys. J. *71*, 561–575.

Berman, H.M., Westbrook, J., Feng, Z., Gilliland, G., Bhat, T.N., Weissig, H., Shindyalov, I.N., and Bourne, P.E. (2000). The Protein Data Bank. Nucleic Acids Res. *28*, 235–242.

Bittova, L., Sumandea, M., and Cho, W. (1999). A structure-function study of the C2 domain of cytosolic phospholipase $A_2$. J. Biol. Chem. *274*, 9665–9672.

Bock, J.B., Klumperman, J., Davanger, S., and Scheller, R.H. (1997). Syntaxin 6 functions in trans-Golgi network vesicle trafficking. Mol. Biol. Cell *8*, 1261–1271.

Bolsover, S.R., Gomez-Fernandez, J.C., and Corbalan-Garcia, S. (2003). Role of the $Ca^{2+}$/phosphatidylserine-binding region of the C2 domain in the translocation of Protein Kinase C alpha to the plasma membrane. J. Biol. Chem. *278*, 10282–10290.

Brooks, B.R., Bruccoleri, R.E., Olafson, B.D., States, D.J., Swaminathan, S., and Karplus, M. (1983). CHARMM: a program for macromolecular energy, minimization, and dynamics calculations. J. Comp. Chem. *4*, 187–217.

Brown, W.J., Chambers, K., and Doody, A. (2003). Phospholipase $A_2$ ($PLA_2$) Enzymes in membrane trafficking: mediators of membrane shape and function. Traffic *4*, 214–221.

Buckland, A.G., and Wilton, D.C. (1998). Inhibition of human cytosolic phospholipase $A_2$ by human annexin V. Biochem. J. *329*, 369–372.

Chae, Y.K., Abildgaard, F., Chapman, E.R., and Markley, J.L. (1998). Lipid binding ridge on loops 2 and 3 of the C2A domain of synaptotagmin I as revealed by NMR spectroscopy. J. Biol. Chem. *273*, 25659–25663.

Chapman, E.R., and Davis, A.F. (1998). Direct interaction of a $Ca^{2+}$-binding loop of synaptotagmin with lipid bilayers. J. Biol. Chem. *273*, 13995–14001.

Chapman, E.R., Hanson, P.I., An, S., and Jahn, R. (1995). $Ca^{2+}$ regulates the interaction between synaptotagmin and syntaxin 1. J. Biol. Chem. *270*, 23667–23671.

Chapman, E.R., and Jahn, R. (1994). Calcium-dependent interaction of the cytoplasmic region of synaptotagmin with membranes. Autonomous function of a single C2-homologous domain. J. Biol. Chem. *269*, 5735–5741.

Chege, N.W., and Pfeffer, S.R. (1990). Compartmentation of the Golgi complex: brefeldin-A distinguishes trans-Golgi cisternae from the trans-Golgi network. J. Cell Biol. *111*, 893–899.

Choukroun, G.J., Marshansky, V., Gustafson, C.E., McKee, M., Hajjar, R.J., Rosenzweig, A., Brown, D., and Bonventre, J.V. (2000). Cytosolic phospholipase $A_2$ regulates Golgi structure and modulates intracellular trafficking of membrane proteins. J. Clin. Investig. *106*, 983–993.

Conesa-Zamora, P., Lopez-Andreo, M.J., Gomez-Fernandez, J.C., and Corbalan-Garcia, S. (2001). Identification of the phosphatidylserine binding site in the C2 domain that is important for PKC alpha activation and in vivo cell localization. Biochemistry *40*, 13898–13905.

Corbalán-García, S., García-García, J., Rodríguez-Alfaro, J.A., and Gómez-Fernández, J.C. (2003). A new phosphatidylinositol 4,5-bisphosphate-binding site located in the C2 domain of protein kinase C$\alpha$. J. Biol. Chem. *278*, 4972–4980.

Corbalán-García, S., Rodríguez-Alfaro, J.A., and Gómez-Fernández, J.C. (1999). Determination of the calcium-binding sites of the C2 domain of protein kinase C$\alpha$ that are critical for its translocation to the plasma membrane. Biochem. J. *337*, 513–521.

Davletov, B., Perisic, O., and Williams, R.L. (1998). Calcium-dependent membrane penetration is a hallmark of the C2 domain of cytosolic phospholipase $A_2$ whereas the C2A domain of synaptotagmin binds membranes electrostatically. J. Biol. Chem. *273*, 19093–19096.

Davletov, B.A., and Sudhof, T.C. (1993). A single C2 domain from synaptotagmin I is sufficient for high affinity $Ca^{2+}$/phospholipid binding. J. Biol. Chem. *268*, 26386–26390.

Dessen, A., Tang, J., Schmidt, H., Stahl, M., Clark, J.D., Seehra, J., and Somers, W.S. (1999). Crystal structure of human cytosolic phospholipase $A_2$ reveals a novel topology and catalytic mechanism. Cell *97*, 349–360.

Dowler, S., Currie, R.A., Campbell, D.G., Deak, M., Kular, G., Downes, C.P., and Alessi, D.R. (2000). Identification of pleckstrin-homology-domain-containing proteins with novel phosphoinositide-binding specificities. Biochem. J. *351*, 19–31.

Ellenberg, J., Siggia, E.D., Moreira, J.E., Smith, C.L., Presley, J.F., Worman, H.J., and Lippincott-Schwartz, J. (1997). Nuclear membrane dynamics and reassembly in living cells: targeting of an inner nuclear membrane protein in interphase and mitosis. J. Cell Biol. *138*, 1193–1206.

Evans, J.H., Fergus, D.J., and Leslie, C.C. (2003). Regulation of cytosolic phospholipase $A_2$ translocation. Adv. Enzyme Regul. *43*, 229–244.

Evans, J.H., Spencer, D.M., Zweifach, A., and Leslie, C.C. (2001). Intracellular calcium signals regulating cytosolic phospholipase $A_2$ translocation to internal membranes. J. Biol. Chem. *276*, 30150–30160.

Frazier, A.A., Roller, C.R., Havelka, J.J., Hinderliter, A., and Cafiso, D.S. (2003). Membrane-bound orientation and position of the synaptotagmin I C2A domain by site-directed spin labeling. Biochemistry *42*, 96–105.

Frazier, A.A., Wisner, M.A., Malmberg, N.J., Victor, K.G., Fanucci, G.E., Nalefski, E.A., Falke, J.J., and Cafiso, D.S. (2002). Membrane orientation and position of the C2 domain from $cPLA_2$ by site-directed spin labeling. Biochemistry *41*, 6282–6292.

Fricker, M., Hollinshead, M., White, N., and Vaux, D. (1997). Interphase nuclei of many mammalian cell types contain deep, dynamic, tubular membrane-bound invaginations of the nuclear envelope. J. Cell Biol. *136*, 531–544.

Funk, C.D. (2001). Prostaglandins and leukotrienes: advances in eicosanoid biology. Science *294*, 1871–1875.

Geppert, M., Goda, Y., Hammer, R.E., Li, C., Rosahl, T.W., Stevens, C.F., and Sudhof, T.C. (1994). Synaptotagmin I: a major $Ca^{2+}$ sensor for transmitter release at a central synapse. Cell *79*, 717–727.

Gerber, S.H., Rizo, J., and Sudhof, T.C. (2001). The top loops of the C2 domains from synaptotagmin and phospholipase $A_2$ control functional specificity. J. Biol. Chem. *276*, 32288–32292.

Gijón, M.A., Spencer, D.M., Kaiser, A.L., and Leslie, C.C. (1999). Role of phosphorylation sites and the C2 domain in regulation of cytosolic phospholipase $A_2$. J. Cell Biol. *145*, 1219–1232.

Gkantiragas, I., Brugger, B., Stuven, E., Kaloyanova, D., Li, X.Y., Lohr, K., Lottspeich, F., Wieland, F.T., and Helms, J.B. (2001). Sphingomyelin-enriched microdomains at the Golgi complex. Mol. Biol. Cell *12*, 1819–1833.

Glover, S., de Carvalho, M.S., Bayburt, T., Jonas, M., Chi, E., Leslie, C.C., and Gelb, M.H. (1995). Translocation of the 85-kDa phospholipase $A_2$ from cytosol to the nuclear envelope in rat basophilic leukemia cells stimulated with calcium ionophore or IgE/antigen. J. Biol. Chem. *270*, 15359–15367.

Griesbeck, O., Baird, G.S., Campbell, R.E., Zacharias, D.A., and Tsien, R.Y. (2001). Reducing the environmental sensitivity of yellow fluorescent protein. Mechanism and applications. J. Biol. Chem. *276*, 29188–29194.

Hirabayashi, T., Kume, K., Hirose, K., Yokomizo, T., Iino, M., Itoh, H., and Shimizu, T. (1999). Critical duration of intracellular $Ca^{2+}$ response required for continuous translocation and activation of cytosolic phospholipase $A_2$. J. Biol. Chem. *274*, 5163–5169.

Hixon, M.S., Ball, A., and Gelb, M.H. (1998). Calcium-dependent and -independent interfacial binding and catalysis of cytosolic group IV phospholipase $A_2$. Biochemistry *37*, 8516–8526.

Huwiler, A., Johansen, B., Skarstad, A., and Pfeilschifter, J. (2001). Ceramide binds to the CaLB domain of cytosolic phospholipase $A_2$ and facilitates its membrane docking and arachidonic acid release. FASEB J. *15*, 7–9.

Itoh, T., and Takenawa, T. (2002). Phosphoinositide-binding domains: functional units for temporal and spatial regulation of intracellular signalling. Cell Signal. *14*, 733–743.

Keller, P., Toomre, D., Diaz, E., White, J., and Simons, K. (2001). Multicolour imaging of post-Golgi sorting and trafficking in live cells. Nat. Cell Biol. *3*, 140–149.

Kitatani, K., Oka, T., Murata, T., Hayama, M., Akiba, S., and Sato, T. (2000). Acceleration by ceramide of calcium-dependent translocation of phospholipase $A_2$ from cytosol to membranes in platelets. Arch. Biochem. Biophys. *382*, 296–302.

Kohout, S.C., Corbalan-Garcia, S., Torrecillas, A., Gomez-Fernandez, J.C., and Falke, J.J. (2002). C2 domains of protein kinase C isoforms alpha, beta, and gamma: activation parameters and calcium stoichiometries of the membrane-bound state. Biochemistry *41*, 11411–11424.

Leslie, C.C., and Channon, J.Y. (1990). Anionic phospholipids stimulate an arachidonoyl-hydrolyzing phospholipase $A_2$ from macrophages and reduce the calcium requirement for activity. Biochim. Biophys. Acta *1045*, 261–270.

Lippincott-Schwartz, J., Yuan, L.C., Bonifacino, J.S., and Klausner, R.D. (1989). Rapid redistribution of Golgi proteins into the ER in cells treated with

brefeldin A: evidence for membrane cycling from Golgi to ER. Cell *56*, 801–813.

Maasch, C., Wagner, S., Lindschau, C., Alexander, G., Buchner, K., Gollasch, M., Luft, F.C., and Haller, H. (2000). Protein kinase C alpha targeting is regulated by temporal and spatial changes in intracellular free calcium concentration [$Ca^{2+}$]$_i$. FASEB J. *14*, 1653–1663.

Mineo, C., Ying, Y.S., Chapline, C., Jaken, S., and Anderson, R.G. (1998). Targeting of protein kinase C alpha to caveolae. J. Cell Biol. *141*, 601–610.

Misura, K.M., Bock, J.B., Gonzalez, L.C., Jr., Scheller, R.H., and Weis, W.I. (2002). Three-dimensional structure of the amino-terminal domain of syntaxin 6, a SNAP-25 C homolog. Proc. Natl. Acad. Sci. USA *99*, 9184–9189.

Mosior, M., Six, D.A., and Dennis, E.A. (1998). Group IV cytosolic phospholipase $A_2$ binds with high affinity and specificity to phosphatidylinositol 4,5-bisphosphate resulting in dramatic increases in activity. J. Biol. Chem. *273*, 2184–2191.

Murray, D., Hermida-Matsumoto, L., Buser, C.A., Tsang, J., Sigal, C.T., Ben-Tal, N., Honig, B., Resh, M.D., and McLaughlin, S. (1998). Electrostatics and the membrane association of Src: theory and experiment. Biochemistry *37*, 2145–2159.

Murray, D., and Honig, B. (2002). Electrostatic control of the membrane targeting of C2 domains. Mol. Cell *9*, 145–154.

Nakatani, Y., Tanioka, T., Sunaga, S., Murakami, M., and Kudo, I. (2000). Identification of a cellular protein that functionally interacts with the C2 domain of cytosolic phospholipase $A_2$ alpha. J. Biol. Chem. *275*, 1161–1168.

Nalefski, E.A., and Falke, J.J. (1996). The C2 domain calcium-binding motif: structural and functional diversity. Protein Sci. *5*, 2375–2390.

Nalefski, E.A., and Falke, J.J. (1998). Location of the membrane-docking face on the $Ca^{2+}$-activated C2 domain of cytosolic phospholipase $A_2$. Biochemistry *37*, 17642–17650.

Nalefski, E.A., and Newton, A.C. (2001). Membrane binding kinetics of protein kinase C betaII mediated by the C2 domain. Biochemistry *40*, 13216–13229.

Nalefski, E.A., Slazas, M.M., and Falke, J.J. (1997). $Ca^{2+}$-signaling cycle of a membrane-docking C2 domain. Biochemistry *36*, 12011–12018.

Nalefski, E.A., Sultzman, L.A., Martin, D.M., Kriz, R.W., Towler, P.S., Knopf, J.L., and Clark, J.D. (1994). Delineation of two functionally distinct domains of cytosolic phospholipase $A_2$, a regulatory $Ca^{2+}$-dependent lipid-binding domain and a $Ca^{2+}$-independent catalytic domain. J. Biol. Chem. *269*, 18239–18249.

Nalefski, E.A., Wisner, M.A., Chen, J.Z., Sprang, S.R., Fukuda, M., Mikoshiba, K., and Falke, J.J. (2001). C2 domains from different $Ca^{2+}$ signaling pathways display functional and mechanistic diversity. Biochemistry *40*, 3089–3100.

Nicholls, A., Sharp, K.A., and Honig, B. (1991). Protein folding and association: insights from the interfacial and thermodynamic properties of hydrocarbons. Proteins *11*, 281–296.

Nishiki, T., Kamata, Y., Nemoto, Y., Omori, A., Ito, T., Takahashi, M., and Kozaki, S. (1994). Identification of protein receptor for Clostridium botulinum type B neurotoxin in rat brain synaptosomes. J. Biol. Chem. *269*, 10498–10503.

Novick, P., and Zerial, M. (1997). The diversity of Rab proteins in vesicle transport. Curr. Opin. Cell Biol. *9*, 496–504.

Oancea, E., and Meyer, T. (1998). Protein kinase C as a molecular machine for decoding calcium and diacylglycerol signals. Cell *95*, 307–318.

Ochoa, W.F., Corbalan-Garcia, S., Eritja, R., Rodriguez-Alfaro, J.A., Gomez-Fernandez, J.C., Fita, I., and Verdaguer, N. (2002). Additional binding sites for anionic phospholipids and calcium ions in the crystal structures of complexes of the C2 domain of protein kinase Calpha. J. Mol. Biol. *320*, 277–291.

Perisic, O., Fong, S., Lynch, D.E., Bycroft, M., and Williams, R.L. (1998). Crystal structure of a calcium-phospholipid binding domain from cytosolic phospholipase $A_2$. J. Biol. Chem. *273*, 1596–1604.

Perisic, O., Paterson, H.F., Mosedale, G., Lara-González, S., and Williams, R.L. (1999). Mapping the phospholipid-binding surface and translocation determinants of the C2 domain from cytosolic phospholipase $A_2$. J. Biol. Chem. *274*, 14979–14987.

Rizo, J., and Sudhof, T.C. (1998). C2-domains, structure and function of a universal $Ca^{2+}$-binding domain. J. Biol. Chem. *273*, 15879–15882.

Sali, A., and Blundell, T.L. (1993). Comparative protein modelling by satisfaction of spatial restraints. J. Mol. Biol. *234*, 779–815.

Sato, T., Kageura, T., Hashizume, T., Hayama, M., Kitatani, K., and Akiba, S. (1999). Stimulation by ceramide of phospholipase $A_2$ activation through a mechanism related to the phospholipase C-initiated signaling pathway in rabbit platelets. J. Biochem. *125*, 96–102.

Schiavo, G., Gu, Q.M., Prestwich, G.D., Sollner, T.H., and Rothman, J.E. (1996). Calcium-dependent switching of the specificity of phosphoinositide binding to synaptotagmin. Proc. Natl. Acad. Sci. USA *93*, 13327–13332.

Schievella, A.R., Regier, M.K., Smith, W.L., and Lin, L.-L. (1995). Calcium-mediated translocation of cytosolic phospholipase $A_2$ to the nuclear envelope and endoplasmic reticulum. J. Biol. Chem. *270*, 30749–30754.

Sciaky, N., Presley, J., Smith, C., Zaal, K.J., Cole, N., Moreira, J.E., Terasaki, M., Siggia, E., and Lippincott-Schwartz, J. (1997). Golgi tubule traffic and the effects of brefeldin A visualized in living cells. J. Cell Biol. *139*, 1137–1155.

Shao, X., Fernandez, I., Sudhof, T.C., and Rizo, J. (1998). Solution structures of the $Ca^{2+}$-free and $Ca^{2+}$-bound C2A domain of synaptotagmin I: does $Ca^{2+}$ induce a conformational change? Biochemistry *37*, 16106–16115.

Shao, X., Li, C., Fernandez, I., Zhang, X., Sudhof, T.C., and Rizo, J. (1997). Synaptotagmin-syntaxin interaction: the C2 domain as a $Ca^{2+}$-dependent electrostatic switch. Neuron *18*, 133–142.

Sharp, K.A., and Honig, B.H. (1990). Calculating total electrostatic energies with the nonlinear Poisson-Boltzmann equation. J. Phys. Chem. *94*, 7684–7692.

Sheridan, A.M., Force, T., Yoon, H.J., O'Leary, E., Choukroun, G., Taheri, M.R., and Bonventre, J.V. (2001). PLIP, a novel splice variant of Tip60, interacts with group IV cytosolic phospholipase $A_2$, induces apoptosis, and potentiates prostaglandin production. Mol. Cell Biol. *21*, 4470–4481.

Shindyalov, I.N., and Bourne, P.E. (1998). Protein structure alignment by incremental combinatorial extension (CE) of the optimal path. Protein Eng. *11*, 739–747.

Six, D.A., and Dennis, E.A. (2003). Essential $Ca^{2+}$-independent role of the group IVA cytosolic phospholipase $A_2$ C2 domain for interfacial activity. J. Biol. Chem.

Solito, E., Raguenes-Nicol, C., de Coupade, C., Bisagni-Faure, A., and Russo-Marie, F. (1998). U937 cells deprived of endogenous annexin 1 demonstrate an increased $PLA_2$ activity. Br. J. Pharmacol. *124*, 1675–1683.

Stahelin, R.V., Rafter, J.D., Das, S., and Cho, W. (2003). The molecular basis of differential subcellular localization of C2 domains of protein kinase C-alpha and group IVa cytosolic phospholipase $A_2$. J. Biol. Chem. *278*, 12452–12460.

Stauffer, T.P., Ahn, S., and Meyer, T. (1998). Receptor-induced transient reduction in plasma membrane PtdIns(4, 5)$P_2$ concentration monitored in living cells. Curr. Biol. *8*, 343–346.

Sudhof, T.C., and Rizo, J. (1996). Synaptotagmins: C2-domain proteins that regulate membrane traffic. Neuron *17*, 379–388.

Sugita, S., and Sudhof, T.C. (2000). Specificity of $Ca^{2+}$-dependent protein interactions mediated by the C2A domains of synaptotagmins. Biochemistry *39*, 2940–2949.

Sutton, R.B., Davletov, B.A., Berghuis, A.M., Sudhof, T.C., and Sprang, S.R. (1995). Structure of the first C2 domain of synaptotagmin I: a novel $Ca^{2+}$/phospholipid-binding fold. Cell *80*, 929–938.

Teruel, M.N., and Meyer, T. (2000). Translocation and reversible localization of signaling proteins: a dynamic future for signal transduction. Cell *103*, 181–184.

Teruel, M.N., and Meyer, T. (2002). Parallel single-cell monitoring of receptor-triggered membrane translocation of a calcium-sensing protein module. Science *295*, 1910–1912.

Varnai, P., and Balla, T. (1998). Visualization of phosphoinositides that bind pleckstrin homology domains: calcium- and agonist-induced dynamic changes and relationship to myo-[$^3$H]inositol-labeled phosphoinositide pools. J. Cell Biol. *143*, 501–510.

Verdaguer, N., Corbalan-Garcia, S., Ochoa, W.F., Fita, I., and Gomez-Fernandez, J.C. (1999). $Ca^{2+}$ bridges the C2 membrane-binding domain of protein kinase C alpha directly to phosphatidylserine. EMBO J. *18*, 6329–6338.

Watt, S.A., Kular, G., Fleming, I.N., Downes, C.P., and Lucocq, J.M. (2002). Subcellular localization of phosphatidylinositol 4,5-bisphosphate using the pleckstrin homology domain of phospholipase C delta1. Biochem. J. *363*, 657–666.

Xu, G.-Y., McDonagh, T., Hsiang-Ai, Y., Nalefski, E.A., Clark, J.D., and Cumming, D.A. (1998). Solution structure and membrane interactions of the C2 domain of cytosolic phospholipase $A_2$. J. Mol. Biol. *280*, 485–500.

Zhang, X., Rizo, J., and Sudhof, T.C. (1998). Mechanism of phospholipid binding by the C2A-domain of synaptotagmin I. Biochemistry *37*, 12395–12403.